CALIFORNIA INSTITUTE OF TECHNOLOGY

SOIL MECHANICS LABORATORY

AN INTEGRATED APPROACH TO THE STRESS ANALYSIS OF GRANULAR MATERIALS

by

T. Y. Chang, H. Y. Ko, R. F. Scott
and R. A. Westmann

A report on research conducted for the
National Science Foundation

Pasadena, California

1967

AN INTEGRATED APPROACH TO THE STRESS ANALYSIS OF GRANULAR MATERIALS

by

T. Y. Chang, H. Y. Ko, R. F. Scott
and R. A. Westmann

A report on research conducted for the
National Science Foundation

Pasadena, California
1967

TABLE OF CONTENTS

I. INTRODUCTION

Up to a very recent time, it has been difficult or impossible to perform exact analyses of any realistic field problem in soil mechanics or soil engineering even when a linearly elastic behavior was assumed for the soil involved. As a consequence, analyses in soil mechanics have been restricted to extremely idealized physical situations including linearly elastic behavior (uniform loads or rigid footings at the surface of semi-infinite elastic continua, for example) or to problems of plastic equilibrium. The latter also include greatly simplified geometries and an idealized material behavior. In part, because of these mathematical difficulties, little attention has been paid in soil mechanics to the deformational properties of soil other than at failure, or for the purpose of getting equivalent elastic moduli.

However, the development of finite or discrete element calculational techniques, along with the availability of large digital computers has enabled useful answers to be obtained to a range of practical structural problems in the last few years. So far, these developments have been mostly employed in the analysis of metal structures[1, 2, 3, 4] for which the assumption of linear

---

[1] J. L. Swedlow and W. H. Yang, "Stiffness Analysis of Elasto-Plastic Plates," GALCIT SM65-10, January, 1966, Firestone Flight Sciences Laboratory, California Institute of Technology, Pasadena, California.

[2] J. H. Argyris, "Elasto-Plastic Matrix Displacement Analysis of Three-Dimensional Continua," J. Roy. Aeronautical Soc., Vol. 69, Sept. 1965, pp. 633-636.

[3] R. W. Clough, "The Finite Element Method in Plane Stress Analysis," Proceedings, ASCE, 2nd Conference on Electronic Computation, Pittsburgh, Pa., September, 1960.

[4] C. W. McCormick, "Plane Stress Analysis," Journal of the Structural Division, ASCE, Vol. 89, August 1963, pp. 37-54.

elasticity may represent a reasonable approximation to the real material behavior.

When it comes to applying these numerical techniques to problems of soil stressing and deformation, it seems highly desirable to utilize the flexibility of the calculational method to the full by including as realistic a material behavior as possible. This is particularly important since the nonlinearities of soil stress-strain behavior have long been recognized, although the knowledge has not been systematized. A review of the literature of soil mechanics affords little guidance in the matter of selecting either linear or nonlinear soil characteristics for use in a given problem. It therefore appears that, for the first time, our ability to make calculations in soil mechanics is outstripping our knowledge of the material properties to be included in the analysis.

For this reason, a program of examining in detail the stress-strain behavior of one granular soil (Ottawa sand) under as homogeneous stress conditions as could be achieved was initiated several years ago. The studies which were made have clarified our understanding of the behavior of this material up to and including yield[5, 6, 7], but have yet to be generalized to other soils.

---

[5] H. Y. Ko and R. F. Scott, "A New Soil Testing Apparatus," Géotechnique, 17, 40-57, March, 1967.

[6] H. Y. Ko and R. F. Scott, "Deformation of Sand in Hydrostatic Compression," Proceedings, ASCE, Journal S. Mech. and Found. Div., SM3, May, 1967, p. 137.

[7] H. Y. Ko and R. F. Scott, "Deformation of Sand in Shear," Proceedings, ASCE, Journal S. Mech. and Found. Div., 1967.

In particular the nonlinear aspects of soil behavior were examined. The important effects, which must be included in any mathematical description of the soil's behavior, are:

(a) nonlinear, but elastic, volume change with hydrostatic stress[6];

(b) nonlinear, partly elastic shearing deformations under applied shearing stresses[7];

(c) the occurrence of volume changes during shearing at constant hydrostatic stress[7].

In addition, the homogeneous stress tests showed that yielding[7] occurred at much smaller strains (generally less than 2% principal axial strain) than are encountered in conventional soil test apparatus, which subjects the soil to nonhomogeneous stresses. It was apparent that the important nonlinear aspects of the soil's behavior were developed at small strains, and, within the range of test conditions, were rate-independent, so that it appeared valid to attempt to construct a small-strain nonlinear elastic theory to represent the soil behavior.

Because of the well-developed body of knowledge in the field of solid mechanics on nonlinear small-strain theory[8, 9, 10], it was decided to make the first attempt at describing the observed deformational behavior of the

---

[8] E. Sternberg, "Nonlinear Theory of Elasticity with Small Deformations," Trans. ASME, Vol. 68, Part 2, 1946, pp. A53-A60.

[9] H. Kauderer, Nichtlineare Mechanik, Springer-Verlag, 1958.

[10] R. J. Evans and K. S. Pister, Constitutive Equations for a Class of Nonlinear Elastic Solids, Int. J. of Solids and Structures, Vol. 2, No. 3, July 1966, pp. 427-446.

Ottawa sand at one void ratio by means of a constitutive law for an equivalent continuum. An alternative approach is, of course, to determine a rational model for the soil's behavior based on the mechanics of the interaction of the particles, and, in fact, some success was obtained with this method in explaining the hydrostatic behavior of the material[6]. However, the extension to general deformational behavior is not easy, and the continuum approach was therefore tested first.

As explained in this report, a second-order nonlinear elastic constitutive law is established for a continuum, with the idea that the selection of appropriate material constants will give rise to a model continuum whose macroscopic behavior will be closely similar to that of the real soil. Because of the behavior of the real soil on unloading, its behavior is only simulated on loading paths. An attempt at constructing a constitutive law in this way is only worthwhile on the basis of soil tests in which very nearly homogeneous stress and strain conditions have been achieved. In parallel with the development of the appropriate theory, the numerical analysis leading to the writing of a finite element computer program was undertaken to deal with field problems in a model nonlinear continuum of the desired properties. The material tests, nonlinear theory, model properties, and computer program were all finally coalesced in the solution of a sample problem.

This total effort required the abilities of a group of investigators of diverse but overlapping interests; the interaction was a stimulating and educating experience.

II. FUNDAMENTAL FORMULATIONS

In the following it is assumed that the soil material can be satisfactorily modeled by a continuum. The properties of the continuum are to be determined so its response is identical with the statistical response of the soil. No attempt is made to determine the details of particle-to-particle action except at the statistical level predicted from the continuum model.

In the next section the basic field equations of continuum mechanics are reviewed. This is followed by a brief introduction to the constitutive equation theory of nonlinear elasticity. The convention of continuum mechanics is followed whereby tensile stresses are positive, and compressive negative.

1. Field Equations

Employing the usual index notation, the Cartesian components u_i in the coordinate directions x_j of the displacement vector field of the continuum are denoted by

$$u_i = u_i(x_j) \qquad i, j = 1, 2, 3$$

As pointed out in the introduction, attention will be devoted to problems in which the gradient of the displacement vector is small, i.e. $\left| \frac{\partial u_i}{\partial x_j} \right| << 1$. The deformation is then determined in terms of the strain tensor, components of which ϵ_{ij}, are given in terms of the displacement field by the relations

$$\epsilon_{ij} = \frac{1}{2} \left(\frac{\partial u_i}{\partial x_j} + \frac{\partial u_j}{\partial x_i} \right) \qquad (1)$$

The components of the stress tensor are denoted by τ_{ij}. As only static problems are to be considered the stress components must satisfy the equilibrium relations

$$\frac{\partial \tau_{ij}}{\partial x_j} + F_i = 0 \tag{2}$$

where F_i are the components of the known body forces. In addition, boundary conditions must be enforced. These will be taken to be either the prescription of the boundary displacements U_i

$$u_i(x_j) = U_i(x_j) \qquad x_j \text{ on boundary} \tag{3a}$$

or surface tractions T_i

$$\tau_{ij} n_j = T_i \qquad x_j \text{ on boundary, } n_j \text{ unit normal vector to boundary} \tag{3b}$$

2. Constitutive Equations

The chief characteristics of the soil stress-strain relations have been summarized in the introduction. A constitutive law completely describing the entire range of soil behavior would necessarily have to be of the incremental type[11]. This approach will not be adopted here, but instead attention will be restricted to problems in which the applied loads are monotonically increasing. With this restriction a nonlinear deformation law may be successfully employed.

The development of a deformation law might proceed in several ways. It should be emphasized, though, that the final stress-strain

---

[11] R. Hill, The Mathematical Theory of Plasticity, Oxford Press, 1950.

[12] B. Budiansky, "A Reassessment of Deformation Theories of Plasticity," Journal of Applied Mechanics, Vol. 26, 1959, pp. 259-264.

relations must be true constitutive laws valid for all stress states, subject only to the restrictions common to deformation laws[12]. In the following the soil is modeled by a nonlinear elastic continuum. This does not imply that the soil is elastic but only that, when it is subjected to monotonically increasing load applications, the soil behaves just like a particular nonlinear elastic material. The difference between the granular material and its nonlinear elastic model will only be revealed upon release of the applied loads. However, this aspect will not be considered at this time.

Two fundamental methods of formulating nonlinear elastic stress-strain relations are due to Green and Cauchy[13] respectively. These will be developed in parallel below for comparison purposes, since each approach has certain advantages. The method due to Green postulates the existence of a strain energy density function W for the model continuum. To represent a material that is initially isotropic and to satisfy requirements of objectivity, the strain energy can be taken to be a function of any three independent strain invariants, I_1, I_2, I_3

$$W = W(I_1, I_2, I_3) .$$

Here we define the invariants as follows:

$$I_1 = \epsilon_{ii}$$

$$I_2 = \frac{1}{2} \epsilon_{ij} \epsilon_{ij}$$

$$I_3 = \frac{1}{3} \epsilon_{i\ell} \epsilon_{\ell j} \epsilon_{ji} .$$

---

[13] A. C. Eringen, Nonlinear Theory of Continuous Media, McGraw-Hill, 1962.

For an adiabatic process, conservation of energy requires that

$$\tau_{ij} = \frac{\partial W}{\partial \epsilon_{ij}} = \frac{\partial W}{\partial I_1}\,\delta_{ij} + \frac{\partial W}{\partial I_2}\,\epsilon_{ij} + \frac{\partial W}{\partial I_3}\,\epsilon_{i\ell}\,\epsilon_{\ell j} \tag{4}$$

where δ_{ij} is the Kronecker delta. This leads to the desired stress-strain relation.

In Cauchy's method it is simply postulated that the state of stress is a function of the current state of strain

$$\tau_{ij} = f_{ij}(\epsilon_{k\ell})$$

For an isotropic material and a restricted class of functions, f_{ij} may be expanded to yield

$$\tau_{ij} = \alpha_o \delta_{ij} + \alpha_1 \epsilon_{ij} + \alpha_2 \epsilon_{i\ell}\epsilon_{\ell j} + \alpha_3 \epsilon_{i\ell}\epsilon_{\ell k}\epsilon_{kj} + \cdots \tag{5}$$

where

$$\alpha_m = \alpha_m(I_1, I_2, I_3) \qquad m = 1, 2, 3 \cdots$$

Utilizing the Cayley-Hamilton theorem[14] permits the reduction of (5) to

$$\tau_{ij} = \Psi_o \delta_{ij} + \Psi_1 \epsilon_{ij} + \Psi_2 \epsilon_{i\ell}\epsilon_{\ell j} \tag{6}$$

where

$$\Psi_i = \Psi_i(I_1, I_2, I_3)$$

are material coefficients to be determined. Note that Eq. (6) is the same general form as given by Eq. (4).

The problem statement is now complete. For the given material and material coefficients, Eqs. (1), (2), and (4) or (6) must be solved subject

---

[14] W. Prager, Introduction to Mechanics of Continua, Ginn and Co., 1961.

to the boundary conditions, Eqs. (3). The solution leads to the stress and displacement fields in the model continuum which then must be interpreted in terms of the real granular material.

III. MATERIAL CHARACTERIZATION

In this section special forms of the general constitutive laws are presented and their suitability for representing a granular material is discussed. In preparation for subsequent numerical work incremental stress-strain laws are deduced. Solutions for material tests are presented, and, using these test results, material constants are determined. Evaluation of the proposed constitutive law is then made by comparing the derived stress-strain relations with the true material behavior.

1. Second Order Approximation

In the introduction some of the special characteristics of the stress-strain relations for granular materials were pointed out. It is the purpose here to develop a simple stress-strain law that can at least qualitatively account for the three most important observations: nonlinear pressure-volume change relation, nonlinear shear effect and the shear-dilatancy coupling.

Possibly the simplest approach is to expand the unknown functions of the strain invariants in polynomials of the strains (or strain invariants) retaining only polynomial terms up to a certain order[13(page 168) 15]. If in the final stress-strain relation only terms in strain up to second power are retained, the relation is called a second order approximation. It is our purpose here to seek the lowest order approximation which will still

---

[15] R. J. Evans, Constitutive Equations for a Class of Nonlinear Elastic Solids, Report No. 65-5, Structures and Materials Research, Department of Civil Engineering, University of California, Berkeley, June 1965.

represent adequately the observed behavior. Consequently, the second order approximation is examined.

To illustrate this, we express the strain energy function W in terms of all powers of strain up to three:

$$W = A_o + A_1 I_1 + B_1 I_1^2 + B_2 I_1^3 + B_3 I_1 I_2 + B_4 I_2 + B_5 I_3 \tag{7}$$

where B_1, B_2, B_3, B_4, B_5 are material constants to be evaluated from suitable tests*. Substituting into Eq. (4) (Green's method) yields the second order law

$$\tau_{ij} = \left(2B_1 I_1 + 3B_2 I_1^2 + B_3 I_2\right)\delta_{ij} + \left(B_4 + B_3 I_1\right)\epsilon_{ij} + B_5 \epsilon_{i\ell}\epsilon_{\ell j} \tag{8}$$

In a similar process applied to Cauchy's approach, Eq. (6) can be expanded to yield the second order law

$$\tau_{ij} = \left(C_1 I_1 + C_2 I_1^2 + C_3 I_2\right)\delta_{ij} + \left(C_4 + C_5 I_1\right)\epsilon_{ij} + C_6 \epsilon_{i\ell}\epsilon_{\ell j} \tag{9}$$

where again C_1 to C_6 are constants to be experimentally determined. Note that equations (8) and (9) are identical if $C_3 = C_5$. This restriction on the material constants develops from the postulate that a strain energy function exists. This thermodynamic restriction thus reduces the number of constants in the Cauchy approach from six to five.

In the numerical work, it is desirable to have a symmetric stress-strain law since the subsequent computational effort is thereby reduced. As may be readily shown, the stress-strain laws derived by Green's method are automatically symmetric. For this reason Eq. (8) is selected to model the granular material**. If one does not wish to admit the existence of a strain-energy function, then Cauchy's method must be utilized. In

---

*A_o and A_1 are set equal to zero so that a zero strain state corresponds to a zero stress state and a zero strain energy level.

**This does not imply that the granular material has a strain energy function. It only means that the modeling continuum (which behaves like the granular material under monotonically increasing loads) possesses a strain-energy function.

the case of a second order law the desired symmetry is obtained from Eq. (9) by arbitrarily setting $C_3 = C_5$.

It will be demonstrated in § III. 4 that Eq. (8) can qualitatively reproduce the special characteristics of a granular material.

Note that, if in Eq. (8) the second order terms are neglected (or equivalently $B_2 = B_3 = B_5 = 0$), a linear stress-strain relation is recovered. This motivates replacing B_1 and B_4 with the more conventional symbols

$$B_1 = \frac{\lambda}{2} \quad , \quad B_4 = 2\mu$$

where λ and μ are the Lame' elastic constants of linear theory. They can be expressed in terms of Young's modulus E, and Poisson's ratio ν, as follows:

$$\lambda = \frac{\nu E}{(1 + \nu)(1 - 2\nu)}$$

$$\mu = \frac{E}{2(1 + \nu)} \quad .$$

The final form of the stress-strain law then becomes

$$\tau_{ij} = \left(\lambda I_1 + B_2 I_1^2 + B_3 I_2 \right) \delta_{ij} + \left(2\mu + B_3 I_1 \right) \epsilon_{ij} + B_5 \epsilon_{ik} \epsilon_{kj} \qquad (10)$$

2. Incremental Stress-Strain Relations

In preparation for the numerical development, an incremental stress-strain relation is developed from Eq. (10) in the following manner. Suppose an initial strain state ϵ°_{ij} exists with a corresponding stress state τ°_{ij}. If an additional strain increment $\Delta\epsilon_{ij}$ is enforced then the

corresponding stress state becomes $\tau^{\circ}_{ij} + \Delta\tau_{ij}$. From Eq. (10) it follows that

$$\tau^{\circ}_{ij} + \Delta\tau_{ij} = \lambda\left(\epsilon^{\circ}_{mm} + \Delta\epsilon_{mm}\right) + B_2\left(\epsilon^{\circ}_{mm} + \Delta\epsilon_{mm}\right)^2$$
$$+ \frac{B_3}{2}\left(\epsilon^{\circ}_{mn} + \Delta\epsilon_{mn}\right)\left(\epsilon^{\circ}_{mn} + \Delta\epsilon_{mn}\right)\delta_{ij}$$
$$+ \left[2\mu + B_3\left(\epsilon^{\circ}_{mm} + \Delta\epsilon_{mm}\right)\right]\left(\epsilon^{\circ}_{ij} + \Delta\epsilon_{ij}\right)$$
$$+ B_5\left(\epsilon^{\circ}_{i\ell} + \Delta\epsilon_{i\ell}\right)\left(\epsilon^{\circ}_{\ell j} + \Delta\epsilon_{\ell j}\right) \qquad (11)$$

Subtracting the stress-strain relation for the initial state from Eq. (11) leads to the result

$$\Delta\tau_{ij} = \left[\left(\lambda + 2B_2\epsilon^{\circ}_{mm}\right)\delta_{ij} + B_3\epsilon^{\circ}_{ij}\right]\Delta\epsilon_{mm} + \left(2\mu + B_3\epsilon^{\circ}_{mm}\right)\Delta\epsilon_{ij}$$
$$+ B_3\epsilon^{\circ}_{mn}\Delta\epsilon_{mn}\delta_{ij} + B_5\left(\epsilon^{\circ}_{i\ell}\Delta\epsilon_{\ell j} + \epsilon^{\circ}_{\ell j}\Delta\epsilon_{i\ell}\right)$$
$$+ \left\{\left\{\left[B_2\left(\Delta\epsilon_{mm}\right)^2 + \frac{B_3}{2}\Delta\epsilon_{mn}\Delta\epsilon_{mn}\right]\delta_{ij} + \right.\right.$$
$$\left.\left. + B_3\Delta\epsilon_{mm}\Delta\epsilon_{ij} + B_5\Delta\epsilon_{i\ell}\Delta\epsilon_{\ell j}\right\}\right\} \qquad (12)$$

Provided the strain increment is sufficiently small, the second order terms in the strain increments are negligible compared to the first order terms. Neglecting these reduces Eq. (12) to the desired linear incremental stress-strain law

$$\Delta\tau_{ij} = D_{ijk\ell}\,\Delta\epsilon_{k\ell} \qquad (13)$$

where

$$D_{ijk\ell} = \left(\lambda + 2B_2\epsilon^{\circ}_{mm}\right)\delta_{ij}\delta_{k\ell} + \left(2\mu + B_3\epsilon^{\circ}_{mm}\right)\delta_{ik}\delta_{j\ell}$$

$$+ B_3\left(\epsilon^{\circ}_{ij}\delta_{k\ell} + \epsilon^{\circ}_{k\ell}\delta_{ij}\right) + B_5\left(\epsilon^{\circ}_{ik}\delta_{j\ell} + \epsilon^{\circ}_{\ell j}\delta_{ik}\right) \qquad (14)$$

Note that when the initial stress state is zero, Eq. (14) reduces to its isotropic form

$$D_{ijk\ell} = \lambda\delta_{ij}\delta_{k\ell} + 2\mu\,\delta_{ik}\delta_{j\ell}$$

A nonzero initial stress state however leads to an anisotropic material tensor,* a result which is usually referred to as "stress-induced anisotropy."

Finally, it should be pointed out that the initial stress state is usually nonhomogeneous. When this is the case, the initial stress state induces nonhomogeneous stress-strain relations in addition to the anisotropy.

Subsequent numerical work in this study is concerned with the stress-deformation analysis of bodies in a state of plane strain. Accordingly, Eq. (13) is specialized for this particular deformational condition. A state of plane strain is defined to be

$$\epsilon_{\alpha\beta} = \epsilon_{\alpha\beta}(x_\gamma), \quad \epsilon_{\alpha 3} = \epsilon_{33} = 0, \qquad \alpha, \beta, \gamma = 1, 2.$$

Then the strain increments must satisfy the requirement that

$$\Delta\epsilon_{\alpha 3} = \Delta\epsilon_{33} = 0, \qquad \alpha = 1, 2.$$

Substituting into Eq. (13) and considering only the in-plane components of the stress tensor leads to the following relations:

---

*Except in the special case when the initial stress state is hydrostatic.

$$\Delta\tau_{11} = \left[(\lambda + 2\mu) + (2B_2+B_3)\, I_1^{\circ} + 2(B_3+B_5)\, \epsilon_{11}^{\circ} \right] \Delta\epsilon_{11} +$$

$$+ (\lambda+2B_2 I_1^{\circ} + B_3 I_1^{\circ})\, \Delta\epsilon_{22} + 2\epsilon_{12}^{\circ} (B_3+B_5)\, \Delta\epsilon_{12} \qquad (15a)$$

$$\Delta\tau_{22} = \left[\lambda +2B_2 +B_3)I_1^{\circ} \right] \Delta\epsilon_{11} +$$

$$+ \left[(\lambda+2\mu) + (2B_2+B_3)\, I_1^{\circ} + 2(B_3+B_5)\, \epsilon_{22}^{\circ} \right] \Delta\epsilon_{22} +$$

$$+ 2\epsilon_{12}^{\circ} (B_3+B_5)\, \Delta\epsilon_{12} \qquad (15b)$$

$$\Delta\tau_{12} = (B_3+B_5)\, \epsilon_{12}^{\circ} (\Delta\epsilon_{11} + \Delta\epsilon_{22}) + \left[2\mu + (B_3+B_5)\, I_1^{\circ} \right] \Delta\epsilon_{12} \qquad (15c)$$

where $I_1^{\circ} = \epsilon_{11}^{\circ} + \epsilon_{22}^{\circ}$.

Rewriting Eqs. (15) in matrix notation results in the following form for the incremental stress-strain laws for a state of plane strain.

$$\{\Delta\tau\} = [D]\{\Delta\epsilon\} \qquad (16)$$

In Eq. (16) $\{\Delta\tau\}$ and $\{\Delta\epsilon\}$ denote the column vectors

$$\{\Delta\tau\} \begin{Bmatrix} \Delta\tau_{11} \\ \Delta\tau_{22} \\ \Delta\tau_{12} \end{Bmatrix} , \qquad \{\Delta\epsilon\} = \begin{Bmatrix} \Delta\epsilon_{11} \\ \Delta\epsilon_{22} \\ 2\Delta\epsilon_{12} \end{Bmatrix}$$

while the material matrix $[D]$ is given by

$$[D] = \begin{bmatrix} (\lambda+2\mu) + (2B_2+B_3)I_1^{\circ} + 2(B_3+B_5)\epsilon_{11}^{\circ} & \lambda+(2B_2+B_3)I_1^{\circ} & \epsilon_{12}^{\circ}(B_3+B_5) \\ \lambda+(2B_2+B_3)I_1^{\circ} & (\lambda+2\mu)+(2B_2+B_3)I_1^{\circ} + 2(B_3+B_5)\epsilon_{22}^{\circ} & \epsilon_{12}^{\circ}(B_3+B_5) \\ \epsilon_{12}^{\circ}(B_3+B_5) & \epsilon_{12}^{\circ}(B_3+B_5) & 2\mu+(B_3+B_5)I_1^{\circ} \end{bmatrix}$$

Note that the material matrix [D] exhibits the desired symmetry.

3. Limitations of Second Order Law

The second order approximation involves an extension beyond the linear law involving only second order terms. As will be shown in the next section, this is sufficient to at least qualitatively predict the essential features of the granular material behavior. The five material constants must be experimentally determined in order that the second order law best approximate a given material's behavior.

Consider a stress state in which two of the principal strains, ϵ_{II}, ϵ_{III}, are held fixed while ϵ_I is varied. Examination of Eq. (10) reveals that

$$\tau_I = C_o + C_1\epsilon_I + C_2\epsilon_I^2 \tag{17}$$

where τ_I is a principal stress and C_o, C_1, C_2 are constants depending on the material coefficients and the principal strains ϵ_{II}, ϵ_{III}. As shown in Figure 1, Eq. (17) is a parabola with a vertical axis of symmetry. Whether it is concave up or down depends on the material constants. No matter how these constants are chosen the parabolic character of the stress-strain law cannot be altered as long as the second order approximation is retained.

It is quite clear that the second order stress-strain law will be a completely inaccurate model for certain stress states. For example, when the hydrostatic stress is zero, the real granular material cannot support any shearing stresses. In addition it is impossible in a cohesionless granular material to attain a state of hydrostatic tension. Since the second order approximation admits stress states in which the hydrostatic component is zero or positive (hydrostatic tension) the proposed stress-strain law is deficient in this respect.

As illustrated in Figure 1, the stress-strain law exhibits a peak due to its quadratic nature. Depending on the material constants selected, the applicable range of the stress-strain law is generally prior to the extremum ($-\epsilon_I < -\bar{\epsilon}$). However, for analysis purposes, it is necessary to be able to predict when this extremum is reached. Examination of Figure 1 would seem to indicate that this is determined by simply finding the ϵ_I where the slope of the tangent to the $\tau_I - \epsilon_I$ curve vanishes. In practice, it is not as simple as this because in general a three-dimensional stress-state is of interest, not one-dimensional as indicated in Figure 1.

Drucker[16] has presented a stability criterion for the plastic deformation of work-hardening materials. It is found convenient to utilize this concept in determining the point of material instability for the second order law. Drucker's stability postulate states that if a stress state τ_{ij} (with corresponding strain state ϵ_{ij}) is increased by a stress increment $\Delta\tau_{ij}$ (with corresponding strain increment $\Delta\epsilon_{ij}$) then stability requires that

$$\Delta\tau_{ij}\,\Delta\epsilon_{ij} > 0 \tag{18}$$

---

[16] D. C. Drucker, "Variational Principles in the Mathematical Theory of Plasticity," Proceedings of Symposium in Applied Mathematics, Vol. 8, 7-22, 1958.

If $\Delta\tau_{ij}\Delta\epsilon_{ij} = 0$ the extremum point in a three-dimensional state equivalent to Figure 1 has been reached.

The stability criterion can be expressed entirely in terms of the strain increment and material tensor by substituting from Eq. (13) in Eq. (18) to give the requirement

$$D_{ijk\ell}\Delta\epsilon_{ij}\Delta\epsilon_{k\ell} > 0 \tag{19}$$

For the case of plane strain this may be written in the following matrix form:

$$\{\Delta\epsilon\}^T [D]\{\Delta\epsilon\} > 0 \tag{20}$$

where $\{\Delta\epsilon\}$, $[D]$ are defined as in Eq. (16), while $\{\ \}^T$ denotes the transpose of the column vector.

Equation (20) is a real quadratic form. To satisfy the inequality, conditions on $[D]$ [17] are given by

$$D_{11} > 0, \qquad D_{22} > 0, \qquad D_{33} > 0$$

$$\begin{vmatrix} D_{11} & D_{12} \\ D_{12} & D_{22} \end{vmatrix} > 0, \quad \begin{vmatrix} D_{22} & D_{23} \\ D_{23} & D_{33} \end{vmatrix} > 0, \quad \begin{vmatrix} D_{11} & D_{13} \\ D_{13} & D_{33} \end{vmatrix} > 0. \tag{21}$$

where D_{ij} are the components of the material matrix $[D]$.

The components D_{ij} are functions of the current strain-state. Whenever one of the inequalities in Eq. (21) is violated, the material is no longer stable. In the subsequent numerical analysis continual checks must be made to assure the point of material stability is not passed.

---

[17] W. L. Ferrar, Algebra, Oxford, 1957, p. 135.

The constitutive equation appearing in Eq. (10) is a deformation law which equates the total state of stress with the total state of strain. A deformation stress-strain law is not as widely applicable as an incremental law[12]. In the case of proportional loading the deformation law and incremental law are strictly equivalent. Since a stress-strain law is being employed here, we consider proportional straining rather than proportional loading. Proportional straining is defined to be a strain path which produces strain states such that $\epsilon_I : \epsilon_{II} : \epsilon_{III} = \alpha : \beta : 1$ (α, β constants), where ϵ_I, ϵ_{II}, ϵ_{III} are the principal strains. In addition the principal axes are not permitted to rotate. The further restriction has been made in this work that the applied loads are monotonically increasing.

4. Varieties of Tests and Material Constants

Several experiments on a granular material are discussed in this section from the point of view of deriving the material constants from them. In each case, stress-states predicted by the second order law are presented. The representations of these stress states for the different experiments serve two purposes:

(i) They illustrate how the second order law can at least qualitatively predict the essential nonlinear features of the behavior of the granular material.

(ii) They serve as a basis, in conjunction with the experimental results, for measuring the material constants, B_m, as well as assessing the accuracy of the proposed stress-strain law.

Since a deformation law is being used the restriction of proportional straining should be adhered to at least in the determination of the constants.

This implies that a zero state of stress must be taken as a reference state. In the case of granular materials, this is not possible since such a material cannot support any deviatoric stress in the absence of a state of hydrostatic compression. For this reason, a reference stress state of pure hydrostatic compression is taken as the initial state. In the experiments on the material any subsequent deformations added to this initial state satisfy the requirements of proportional straining.

The total deformational state obtained in this way violates the proportional straining rule. It should be pointed out, however, that the reference hydrostatic state is isotropic so that the orientation of the principal axes is not altered during the entire test.

The material tests which will be used to obtain the material properties have been performed on a unique test apparatus capable of independently applying three different principal stresses. The details of the test apparatus and results of typical tests have been presented by Ko and Scott[5]. It is seen from the developments presented above that the nature of the proposed stress-strain law requires strain-controlled tests for property determination. Although basically the test apparatus employed is a stress-controlled device, a slight modification of the test procedure enables certain prescribed strain paths to be achieved.

All of the material data presented herein refers to an Ottawa sand (-20 +40 U.S. sieves) at a void ratio of 0.52. Tests at other void ratios will be required to assess the dependence of the constants obtained on the density of the material.

In the tests to be described in the following paragraphs, proportional straining is involved so that the various principal strain increments $\delta\epsilon_{11}$, $\delta\epsilon_{22}$, etc., can all be expressed in terms of a single strain, usually $\delta\epsilon_{11}$,

which, for the sake of brevity, is expressed as ϵ . Consequently, in the figures which are used to describe the test results and theory, only the strain variable ϵ is shown. This means that $\delta\tau_{22}$, say, in a particular test, is not shown plotted against $\delta\epsilon_{22}$, (which in some tests may be zero) but against the reference control strain ϵ .

In addition, during a test, the increments in the principal stresses and in the corresponding principal strains may increase or decrease compressively, so that, strictly, the stress-strain plots of, say, $\delta\tau_{11}$ versus $\delta\epsilon_{11}$ and $\delta\tau_{22}$ versus $\delta\epsilon_{22}$ should appear in different quadrants of the diagram. This is not done. Instead, all stress-strain data are shown to the right of the stress axis, so that convenient scaling dimensions can be employed. When each diagram is referred to the test it is describing, no confusion need arise.

Hydrostatic Compression

In this particular test the reference state is essentially stress free. Three equal principal strains are applied to the soil sample such that

$$\epsilon_{11} = \epsilon_{22} = \epsilon_{33} = -\epsilon_o \; ; \quad \epsilon_{ij} = 0 \qquad i \neq j$$

From Eq. (12) the corresponding stress state is determined to be

$$\tau_{11} = \tau_{22} = \tau_{33} = -(3\lambda + 2\mu)\epsilon_o + (9B_2 + \frac{9}{2} B_3 + B_5)\epsilon_o^2 \qquad (22)$$

$$\tau_{ij} = 0 \; , \quad i \neq j$$

Equation (22) indicates the capability of the stress-strain law to demonstrate nonlinear behavior in hydrostatic compression. Depending on whether the sign of $9B_2 + \frac{9}{2} B_3 + B_5$ is negative or positive the law predicts a stiffening or softening deviation from a linear response.

In Figure 2, the results from the test are presented. The stiffening effect in volume is readily apparent, implying $9B_2 + \frac{9}{2}B_3 + B_5$ must be negative.

Pure Shear Test

For this test a pure shear plane strain is superposed on a state of hydrostatic compression. The hydrostatic state is then taken to be

$$\epsilon^{\circ}_{11} = \epsilon^{\circ}_{22} = \epsilon^{\circ}_{33} = -b_o$$

$$\epsilon^{\circ}_{ij} = 0 \qquad i \neq j$$

where ϵ°_{ij} denotes the reference state. The superposed state, $\delta\epsilon_{ij}$ is a state of pure shear so

$$\delta\epsilon_{11} = -\epsilon\,, \quad \delta\epsilon_{22} = +\epsilon\,, \quad \delta\epsilon_{33} = 0$$

$$\delta\epsilon_{ij} = 0 \qquad i \neq j$$

Inserting the reference state and superposed state into Eq. (12) gives the following

$$\delta\tau_{11} = -2\mu\epsilon + (3B_3 + 2B_5)b_o\epsilon + (B_3 + B_5)\epsilon^2 \tag{23a}$$

$$\delta\tau_{22} = +2\mu\epsilon - (3B_3 + 2B_5)b_o\epsilon + (B_3 + B_5)\epsilon^2 \tag{23b}$$

$$\delta\tau_{33} = B_5\epsilon^2 \tag{23c}$$

$$\delta\tau_{ij} = 0 \qquad i \neq j \tag{23d}$$

where $\delta\tau_{ij}$ denotes the stress components due to the superposed shear state.

Equations (23a) and (23b) indicate the capability of the second order law to predict nonlinear material performance in shear. Depending on the

sign of $B_3 + B_5$ the material stiffens or softens with increasing shear strain ϵ. Also note that Eqs. (23a) and (23b) predict that the magnitudes of $\delta\tau_{11}$ and $\delta\tau_{22}$ are different by the sign of the term $(B_3+B_5)\epsilon^2$.

Of equal importance is Eq. (23c). Despite the fact the superposed strain state was volume-preserving ($\delta\epsilon_{11} + \delta\epsilon_{22} + \delta\epsilon_{33} = 0$) a normal stress $\delta\tau_{33}$ is predicted. This demonstrates that the proposed second order approximation is capable of accounting for the real material shear-volume change interaction.

In Figure 3 the results of the experiment are presented for an initial hydrostatic strain state of $b_o = 7\times10^{-4}$. Examination of the second terms in Eqs. (23a) and (23b) indicates that the predicted response depends upon the hydrostatic stress. This fact is in qualitative agreement with the real material behavior.

One-Dimensional Confined Compression Test

Again the reference state is taken as hydrostatic compression

$$\epsilon^o_{11} = \epsilon^o_{22} = \epsilon^o_{33} = -b_o$$

$$\epsilon_{ij} = 0 \qquad i \neq j$$

The superposed strain state has only one nonzero component

$$\delta\epsilon_{11} = -\epsilon \ , \qquad \delta\epsilon_{22} = \delta\epsilon_{33} = 0$$

$$\delta\epsilon_{ij} = 0 \qquad i \neq j$$

The stress components measured from the reference state as determined from Eq. (12) are

$$\delta\tau_{11} = -(\lambda+2\mu)\epsilon + (6B_2+5B_3+2B_5)b_o\epsilon + (B_2+\frac{3}{2}B_3+B_5)\epsilon^2 \qquad (24a)$$

$$\delta\tau_{22} = \delta\tau_{33} = -\lambda\epsilon + 2(3B_2 + B_3)\, b_o\epsilon + (B_2 + \frac{B_3}{2})\,\epsilon^2 \tag{24b}$$

$$\delta\tau_{ij} = 0 \qquad i \neq j \tag{24c}$$

The experimental results for this test are presented in Figure 4 for the reference initial strain state $b_o = 2.4 \times 10^{-4}$.

Triaxial Shear Test

This test is quite similar to the pure shear test. The initial state is again taken to be hydrostatic compression

$$\epsilon^o_{11} = \epsilon^o_{22} = \epsilon^o_{33} = -b_o$$

$$\epsilon^o_{ij} = 0 \qquad i \neq j$$

This time though the superposed state is

$$\delta\epsilon_{11} = -\epsilon\,, \qquad \delta\epsilon_{22} = \delta\epsilon_{33} = +\frac{\epsilon}{2}$$

$$\delta\epsilon_{ij} = 0\,, \qquad i \neq j$$

The nonlinear expressions for the stress components resulting from the superposed strains, as determined by Eq. (12), are given by

$$\delta\tau_{11} = -2\mu\epsilon + (3B_3 + 2B_5)b_o\epsilon + (\frac{3}{4}B_3 + B_5)\,\epsilon^2 \tag{25a}$$

$$\delta\tau_{22} = \delta\tau_{33} = +\mu\epsilon - (\frac{3}{2}B_3 + B_5)b_o\epsilon + (\frac{3}{4}B_3 + \frac{B_5}{4})\epsilon^2 \tag{25b}$$

$$\delta\tau_{ij} = 0 \qquad i \neq j \tag{25c}$$

The experimental results arising from this particular test are graphically given in Figure 5 for a reference state $b_o = 5.6 \times 10^{-4}$. It should be pointed out that although this test involves a different strain state than the pure shear test, the essential character of the test is the

same in that it is a state of pure shear strain superposed on a hydrostatic state.

Determination of Material Constants

It remains to so determine the five material constants that the second order law best approximate the real material under test. In each test the second order law predicts a parabolic shape for each stress-strain curve. Accordingly, a tangent or points (or both) may be matched for each curve. An alternative is not to match slopes and points but instead to attempt an evaluation of the material coefficients so that some measure of the overall error is minimized. It is this latter approach that is adopted here. Since this represented the first attempt at a consistent nonlinear representation of soil behavior, a quantitative measure of the matching of the curves was not employed; instead, the constants were adjusted until a reasonable visual fit to the experimental curves was obtained.

Three tests — hydrostatic compression, pure shear and one-dimensional confined compression — were selected in order to determine the constants. In this way the important effects of the stiffening behavior of the material under hydrostatic compression and the softening effect under increasing shear are represented.

By a trial and error procedure the constants were selected so that Eqs. (22), (23a) and (24a) best fit their corresponding experimental curves in Figures 2, 3 and 4 respectively.

Since, for many materials, the ratio λ/μ is close to unity, the two constants λ and μ were taken to be equal, and of such value as to represent approximately the initial portion of the hydrostatic stress-strain curve. The effect of different ratios of λ/μ was examined, and was not

found to be important. When λ and μ had been selected, the other constants which give rise to the nonlinear behavior were chosen to give theoretical curved stress-strain plots following the experimental ones as closely as possible. The resulting values are presented in Table 1. The other equations given above for these tests could have been used instead, and more investigation on the effect of selecting a particular stress-strain curve for fitting purposes has to be done. Examination of the three fitted

TABLE 1.

λ	$= 4.6 \times 10^3$ psi
μ	$= 4.6 \times 10^3$ psi
B_2	$= -1.2 \times 10^6$ psi
B_3	$= -0.2 \times 10^6$ psi
B_5	$= 1.2 \times 10^6$ psi

curves on Figures 2, 3 and 4 reveals a reasonable approximation to the experimental data. In the case of the shear test the predicted curve has a peak at $\epsilon = 0.40\%$ as anticipated in § III. 3.

To determine the overall accuracy of the second order approximation, the other equations (23) through (25) are plotted in Figures 3 through 5 for the material constants of Table 1. In Figure 3 the $\delta\tau_{22}$ curves are only matched for small values of ϵ, the analytical and experimental curves have curvatures of opposite signs and accordingly differ for larger strains. The experimental results indicate that $\delta\tau_{33}$ is essentially zero; the predicted result has the proper initial slope but then deviates considerably

from the horizontal.

In Figure 4 the analytical and experimental results agree fairly well. This is not surprising though since the one-dimensional confined compression test is very similar to the hydrostatic compression test.

Examination of Figure 5 indicates a marked difference between prediction and experiment. This fourth test was not used in the calculation of the constants. If it had the correlation might be expected to be somewhat better. One reason for this discrepancy is possibly due to the fact that the reference hydrostatic states differ in the two tests and the second order law does not properly account for the difference. The predicted response in Figure 5 is "stiffer" than the experimental response, a fact which corresponds to the lower hydrostatic compression in the triaxial shear test.

This points out that the material response depends heavily upon the reference state of hydrostatic compression. To determine the degree of this dependence the same shear tests should be performed at different levels of initial hydrostatic stress. Although tests at different initial states have not been performed to assess this feature, the second order law can at least qualitatively account for this as evidenced by the b_o-terms in Eqs. (23), (24) and (25).

A detailed examination of Figures 2 through 5 indicates that the second order law with the constants from Table 1 only approximates the real material for a limited range of strain states. In any stress analysis using this constitutive law, it cannot be expected that the predicted stress states will agree with their real counterparts for strain states exceeding this limited range.

IV. GENERAL SOLUTION METHOD

The field equations (1), (2), and the constitutive law, Eq. (10), in conjunction with the boundary conditions, Eqs. (3), comprise a complete statement of the nonlinear boundary value problem. The analytical solution to the set of partial differential equations is difficult to obtain except for extremely simple geometries.

Sternberg[8], Kauderer[9] and Evans and Pister[10] have considered problems in elastostatics involving material nonlinearity. The perturbation techniques employed in the works of Kauderer and Evans-Pister depend upon the knowledge of the solution of the corresponding linear problem. In addition, the convergence of the perturbation series is poor for large degrees of nonlinearity.

It is the purpose of this section to present an approximate numerical solution technique that is applicable for a general two-dimensional geometry and large material nonlinearity. The solution method is based upon a piecewise linearization of the constitutive law by applying the loads in increments. Each problem in the resulting sequence of linear problems is solved numerically by the finite element technique which is a numerical scheme based upon the minimization of a functional. This general solution method has been applied earlier by Swedlow and Yang[1] and Argyris[2].

The next subsection is concerned with the development of a variational principle for an initially stressed body. This is followed by an outline of the method of finite elements and the process of incrementing the applied loads. Finally, an estimate of the errors is presented and a simple example completed.

1. Variational Principle

An equivalent statement of the mathematical problem in nonlinear elastostatics may be made in terms of the minimization of a functional. Instead of dealing with a system of nonlinear partial differential equations and boundary conditions, attention is turned to the integral formulation of the problem involving the potential energy of the body.

As stated in[18], the potential energy π of the body is given by

$$\pi = \int_V W(\epsilon_{ij})dV - \int_V F_i u_i dV - \int_{S_1} T_i u_i ds \tag{26}$$

where V is the volume of the body and S_1 that part of the bounding surface on which the surface tractions are prescribed. The terms W, F_i, u_i and T_i have been defined in § II. 1, II. 2. The theorem of minimum potential energy[19] states

> "among all the displacement fields satisfying the geometric boundary conditions, that displacement field which makes the potential energy an absolute minimum satisfies the equilibrium equations and traction boundary conditions."

In this way attention may be focused on the minimization of Eq. (26) as opposed to dealing with Eqs. (1), (2), (3) and (10) directly.

The numerical scheme to be developed is required to deal only with increments of the applied loads. Accordingly, it is necessary to modify the principle of minimum potential energy to permit determination of an incremental state superposed upon a body with an existing stress state.

---

[18] Y. C. Fung, Foundations of Solid Mechanics, Prentice-Hall, 1965.

[19] I. S. Sokolnikoff, Mathematical Theory of Elasticity, McGraw-Hill, 1956.

Consider a body subjected to an equilibrium set of body forces F_i° and surface tractions T_i°. The corresponding initial state is denoted by τ_{ij}°, ϵ_{ij}°, u_i°, π°, W°. Since all of the field equations, constitutive law, and boundary conditions are satisfied

$$\delta\pi^\circ = 0 \tag{27}$$

where the operator $\delta(\ )$ denotes the variation with respect to all admissible displacement fields.

An incremental state, due to ΔF_i, ΔT_i and ΔU_i (on the boundary), is superposed on the initial state. The potential energy then becomes

$$\pi = \pi^\circ + \Delta\pi = \int_V W(\epsilon_{ij}^\circ + \Delta\epsilon_{ij})dV - \int_V (F_i^\circ + \Delta F_i)(u_i^\circ + \Delta u_i)dV$$

$$- \int_{S_1} (T_i^\circ + \Delta T_i)(u_i^\circ + \Delta u_i)ds \tag{27}$$

It is desired to determine the variational principle that governs the induced incremental state $\Delta\tau_{ij}$, $\Delta\epsilon_{ij}$, Δu_i.

Expanding Eq. (27) yields

$$\pi = \int_V W(\epsilon_{ij}^\circ)dV - \int_V F_i^\circ u_i^\circ dV - \int_{S_1} T_i^\circ u_i^\circ ds + \int_V \left(\frac{\partial W}{\partial \epsilon_{ij}}\bigg|_{\epsilon_{ij}^\circ} \Delta\epsilon_{ij} + \frac{\partial^2 W}{\partial\epsilon_{ij}\partial\epsilon_{k\ell}}\bigg|_{\epsilon_{ij}^\circ} \frac{\Delta_{ij}\Delta\epsilon_{k\ell}}{2!} + \cdots\right)dV$$

$$- \int_V (F_i^\circ \Delta u_i + \Delta F_i u_i^\circ + \Delta F_i \Delta u_i)\, dV$$

$$- \int_V (T_i^\circ \Delta u_i + \Delta T_i u_i^\circ + \Delta T_i \Delta u_i)ds \tag{28}$$

The first three integrals in Eq. (28) are simply π°. The Taylor series expansion in the fourth integral may be truncated after the second term

provided the magnitude of the strain increment is sufficiently small.

Upon noting that

$$\left.\frac{\partial W}{\partial \epsilon_{ij}}\right|_{\epsilon^{\circ}_{ij}} = \tau^{\circ}_{ij} \quad , \quad \left.\frac{\partial^2 W}{\partial \epsilon_{ij}\partial \epsilon_{k\ell}}\right|_{\epsilon^{\circ}_{ij}} \Delta\epsilon_{k\ell} = \Delta\tau_{ij} \quad ,$$

we find that Eq. (28) reduces to

$$\pi = \pi^{\circ} + \int_V \left(\tau^{\circ}_{ij} + \frac{\Delta\tau_{ij}}{2}\right)\Delta\epsilon_{ij}\,dV - \int_V \left(F^{\circ}_i \Delta u_i + \Delta F_i u^{\circ}_i + \Delta F_i \Delta u_i\right) dV$$

$$- \int_{S_1} (T^{\circ}_i \Delta u_i + \Delta T_i u^{\circ}_i + \Delta T_i \Delta u_i)\,ds \qquad (29)$$

From the principle of virtual displacements

$$\int_S \tau^{\circ}_{ij}\Delta\epsilon_{ij}\,dV - \int_V F^{\circ}_i \Delta u_i\,dV - \int_{S_1} T^{\circ}_i \Delta u_i\,ds = 0$$

so the potential energy reduces to

$$\pi = \pi^{\circ} + \int_V \frac{1}{2}\Delta\tau_{ij}\Delta\epsilon_{ij}\,dV - \int_V \Delta F_i (u^{\circ}_i + \Delta u_i)\,dV$$

$$- \int_{S_1} \Delta T_i\,(u^{\circ}_i + \Delta u_i)\,ds \qquad (30)$$

The final desired result is obtained by substituting from Eq. (13) for $\Delta\tau_{ij}$ and varying π with respect to all admissible incremental displacement fields* Δu_i. Thus,

*Note that π°, $\Delta T_i u^{\circ}_i$, and $\Delta F_i u^{\circ}_i$ are not dependent on Δu_i.

$$\delta\pi = \delta \left\{ \int_V \left(\frac{1}{2} D_{ijk\ell} \Delta\epsilon_{ij} \Delta\epsilon_{k\ell} - \Delta F_i \Delta u_i \right) dV \right.$$

$$\left. - \int_{S_1} \Delta T_i \Delta u_i ds \right\} = 0 \qquad (31)$$

where $\delta(\ )$ now denotes the variational operator with respect to Δu_i.

2. Finite Element Method

With the appropriate variational principle now established, it is the purpose of this section to outline the development of the numerical solution scheme for the determination of the incremental displacement field Δu_i. The finite element method is based upon a discretization of the displacement field and then minimization of Eq. (31) to determine the unknown components of the displacements.

Consideration is only given to problems involving a state of plane strain. To facilitate the notation the index subscripts are abandoned in favor of two-dimensional x, y coordinates. Accordingly,

$$\Delta u_1, \Delta u_2 \rightarrow \Delta u, \Delta v$$

$$\Delta\epsilon_{11}, \Delta\epsilon_{22}, \Delta\epsilon_{12} \rightarrow \Delta\epsilon_{xx}, \Delta\epsilon_{yy}, \Delta\epsilon_{xy}$$

$$\Delta\tau_{11}, \Delta\tau_{22}, \Delta\tau_{12} \rightarrow \Delta\tau_{xx}, \Delta\tau_{yy}, \Delta\tau_{xy}$$

$$x_1, x_2 \rightarrow x, y$$

$$\Delta F_1, \Delta F_2 \rightarrow \Delta F_x, \Delta F_y$$

$$\Delta T_1, \Delta T_2 \rightarrow \Delta T_x, \Delta T_y$$

To discretize the displacement field the two-dimensional region A is subdivided into M triangular elements* interconnected along element

*Other approaches and element shapes are possible. The method as outlined here is in its simplest form.

interfaces and nodal points as shown in Figure 6. The displacement components at the nodal points serve as the generalized coordinates of the discrete system. A typical triangle shown in Figure 7 has coordinates x_i, y_i, x_j, y_j, x_k, y_k at the i, j, k nodes thus completely describing the shape, size and location of the triangular element.

The incremental displacement field in the m^{th} triangle is taken to have the linear form

$$\Delta u^m(x, y) = c_o + c_1 x + c_2 y \tag{32a}$$

$$\Delta v^m(x, y) = d_o + d_1 x + d_2 y \tag{32b}$$

where c_o through d_2 are constants to be determined. Due to the assumed linearity of the field, compatibility between elements is assured provided adjacent elements have the same displacements at common nodes. This motivates determining the constants so that Δu, Δv evaluated at the nodes are equal to the nodal displacements, i.e.

$$\Delta u^m(x_i, y_i) = \Delta u_i \quad , \quad \Delta v^m(x_i, y_i) = \Delta v_i \tag{33a}$$

$$\Delta u^m(x_j, y_j) = \Delta u_j \quad , \quad \Delta v^m(x_j, y_j) = \Delta v_j \tag{33b}$$

$$\Delta u^m(x_k, y_k) = \Delta u_k \quad , \quad \Delta v^m(x_k, y_k) = \Delta v_k \tag{33c}$$

where* Δu_i, Δv_i are the incremental displacement components in the x- and y-directions, respectively at the i^{th} node.

---

*Note that Δu_i now has different meaning than $\Delta u_i = \Delta u_1, \Delta u_2, \Delta u_3$ (incremental displacements in the coordinate directions) used in earlier sections.

Evaluating the constants c_o through d_2 in this way from Eqs. (33) and substituting v from Eq. (32) into Eq. (1) yields the matrix equation

$$\begin{Bmatrix} \Delta\epsilon_{xx} \\ \Delta\epsilon_{yy} \\ 2\Delta\epsilon_{xy} \end{Bmatrix}^m = \{\Delta\epsilon\}^m = \frac{1}{2a^m}[A]^m\{\Delta u\}^m \tag{34}$$

where the superscript denotes that the m^{th} triangle is involved.

In Eq. (34), $\{\Delta\epsilon\}^m$ is the column strain vector as defined in Eq. (16), while $\{\Delta u\}^m$ denotes

$$\{\Delta u\}^m = \begin{Bmatrix} \Delta u_i \\ \Delta v_i \\ \Delta u_j \\ \Delta v_j \\ \Delta u_k \\ \Delta v_k \end{Bmatrix}$$

which is the column vector of all the nodal displacements of the m^{th} triangular element. In addition $[A]^m$ is the matrix

$$[A]^m = \begin{bmatrix} (y_j-y_k) & 0 & -(y_i-y_k) & 0 & (y_i-y_j) & 0 \\ 0 & -(x_j-x_k) & 0 & (x_i-x_k) & 0 & -(x_i-x_j) \\ -(x_j-x_k) & (y_j-y_k) & (x_i-x_k) & -(y_i-y_k) & -(x_i-x_j) & (y_i-y_j) \end{bmatrix}$$

while a^m is simply the area of the m^{th} triangle

$$a^m = \frac{1}{2}\left[(x_j-x_i)(y_k-y_i) - (x_k-x_i)(y_j-y_i)\right] \quad .$$

Note that the strain state, Eq. (34), is constant throughout the element but of course varies from element to element. The displacement field is continuous throughout the region A of Figure 6 and is completely characterized by the discrete number of nodal displacements. Determination of the nodal displacements immediately fixes the strain field and accordingly the stress field since, from Eqs. (16) and (34)

$$\left\{ \begin{array}{c} \Delta\tau_{xx} \\ \Delta\tau_{yy} \\ \Delta\tau_{xy} \end{array} \right\}^m = \{\Delta\tau\}^m = [D]^m\{\Delta\epsilon\}^m = \frac{1}{2a^m}[D]^m[A]^m\{\Delta u\}^m \qquad (35)$$

The nodal displacements are determined from the variational principle developed in the preceding section. Substituting the results of discretizing the system into Eq. (31) yields

$$\delta\left\{\frac{1}{2}\sum_{m=1}^{M}\iint_A \{\Delta\tau\}^{mT}\{\Delta\epsilon\}^m\,dA - \sum_{m=1}^{M}\iint_A (\Delta F_x\Delta u^m + \Delta F_y\Delta v^m)dA\right.$$

$$\left. - \sum^{N}\int_{S_1}(\Delta T_x\Delta u^m + \Delta T_y\Delta v^m)ds\right\} = 0 \qquad (36)$$

where the area integration is completed over each element separately and M denotes the total number of elements. The surface integral is only carried out on those boundaries on which external tractions are acting; N denotes the number of elements bordering on the boundary S_1. Again $\{\ \}^T$ is the transpose of the column vector.

Completing the first area integration and substituting from Eq. (34) and (35) produces

$$\delta \left\{ \frac{1}{8} \sum_{m=1}^{M} \left(\frac{1}{a_m} \{\Delta u\}^{m^T} [A]^{m^T} [D]^m [A]^m \{\Delta u\}^m \right) \right.$$

$$\left. - \sum_{m=1}^{M} \iint_A (\Delta F_x \Delta u^m + \Delta F_y \Delta v^m) dA - \sum_{S_i}^{N} \int (\Delta T_x \Delta u^m + \Delta T_y \Delta v^m) ds \right\} = 0 \tag{37}$$

The minimization of Eq. (37) is performed with respect to the unknown nodal displacements. The standard procedure in maxima-minima problems in the calculus of several variables requires that

$$\frac{\partial(\ )}{\partial \Delta u_i} = 0 \quad , \quad \frac{\partial(\ )}{\partial \Delta v_i} = 0$$

for all nodal displacements. Completion of the details leads to the matrix equation

$$\begin{bmatrix} K_{11} & K_{12} & \cdot & \cdot & K_{1,2n} \\ K_{21} & K_{22} & \cdot & \cdot & \\ \cdot & & & & \\ \cdot & & & & \\ K_{2n,1} & K_{2n,2} & \cdot & \cdot & K_{2n,2n} \end{bmatrix} \begin{Bmatrix} \Delta u_1 \\ \Delta v_1 \\ \Delta u_2 \\ \cdot \\ \cdot \\ \Delta u_n \\ \Delta v_n \end{Bmatrix} = \begin{Bmatrix} \Delta B_1 \\ \Delta B_2 \\ \cdot \\ \cdot \\ \cdot \\ \Delta B_{2n} \end{Bmatrix} \tag{38}$$

where n is the total number of nodal points.

The stiffness matrix $[K_{ij}]$ arises from the first sum in Eq. (37) while the nonhomogeneous terms $\{\Delta B_i\}$ are due to the incremental body

forces and surface tractions. It is important to note that $[K_{ij}]$ is symmetric, a fact which follows from the symmetry of the material matrix $[D]$, Eq. (16).

Equations (38) are solved for the nodal displacements. Invariably this requires use of a high-speed digital computer. Substitution of the nodal displacements into Eqs. (34) and (35) determines the element stresses and strains thereby completing the solution of the incremental problem.

It should be pointed out that the material matrix $[D]$ depends on the current strain state. Since, in general, the strain state varies from point to point in the body the material matrix is different for each element. In addition, of course, the strain state induces anisotropy in the material. For these reasons the stiffness matrix represents a nonhomogeneous, anisotropic material for each increment.

3. Incremental Deformations

The incremental approach reduces the total nonlinear problem to a series of successive linear problems. This is achieved by subdividing the inputs (body forces, prescribed surface tractions and displacements) into small successive increments. Each input increment is considered to be sufficiently small so the resulting incremental stresses and deformations are related by a linear constitutive law (see § III. 2). This constitutive law is constant during the increment, depending only upon the strain state prior to the increment.

To illustrate how the solution proceeds through successive increments, Eqs.(38) are rewritten

$$[K]_n\{\Delta u\}_n = \{\Delta B\}_n \tag{39}$$

where the subscript* n denotes the n^{th} incremental step.

(i) First Increment

The initial strain-state of the body, and thus the element strains, $\{\epsilon\}_o^m$, must be known. This enables the determination of the material matrix $[D]^m$ from Eq. (16) and then the stiffness matrix $[K]_1$. The loading vector $\{\Delta B\}_1$ is evaluated from the first increments of inputs (body forces, surface tractions or displacements). It is assumed that $\{\Delta B\}_1$ is sufficiently small so that $[D]^m$ (and thus $[K]_1$) are constant during the incremental deformation. It follows from Eq. (39), then, that

$$[K]_1 \{\Delta u\}_1 = \{\Delta B\}_1 \tag{40}$$

Solving Eqs. (40) for $\{\Delta u\}_1$ permits the calculation of the incremental strain and stress state $\{\Delta\epsilon\}_1^m$, $\{\Delta\tau\}_1^m$ for each element from Eqs. (34) and (35).

(ii) Second Increment

The stress and strain increments from the first increment are added to the initial state of the body. This provides the initial known state for the second increment. Since the incremental strains $\{\Delta\epsilon\}_1^m$ most likely vary throughout the body, the material properties are now non-homogeneous and anisotropic (even if the initial state was homogeneous and hydrostatic).

The material matrix for the second increment is determined by substituting the $\{\epsilon\}_o^m + \{\Delta\epsilon\}_1^m$ into Eq. (16), thereby enabling the evaluation of $[K]_2$ from Eq. (37). Again it is assumed the second

---

*At the risk of some confusion, the subscript n on a matrix, $\{\ \}_n$, denotes the increment while a superscript m, $\{\ \}^m$ denotes the element. In the particular case of $\{\Delta u\}_n$ which has no superscript, the vector consists of all the nodal displacements of all elements during the n^{th} increment.

incremental inputs $\{\Delta B\}_2$ are sufficiently small so that $[K]_2$ is essentially constant during the increment. Then we have

$$[K]_2 \{\Delta u\}_2 = \{\Delta B\}_2 \tag{41}$$

Equation (41) is solved for $\{\Delta u\}_2$ which then determines the incremental stresses and strains in the elements, $\{\Delta \epsilon\}_2^m$, $\{\Delta \tau\}_2^m$. The total displacements, stresses and strains $\{u\}^m$, $\{\epsilon\}^m$, $\{\tau\}^m$ are determined by adding all the increments to the initial state:

$$\{u\}^m = \{u\}_o^m + \{\Delta u\}_1^m + \{\Delta u\}_2^m \tag{42a}$$

$$\{\epsilon\}^m = \{\epsilon\}_o^m + \{\Delta \epsilon\}_1^m + \{\Delta \epsilon\}_2 \tag{42b}$$

$$\{\tau\}^m = \{\tau\}_o + \{\Delta \tau\}_1^m + \{\Delta \tau\}_2^m \tag{42c}$$

(iii) Successively higher increments

The third and higher increments proceed as in the case of the second increment. The successive incremental stresses and deformations are added to all the prior increments to obtain the current stress and deformation state.

4. Estimate of Errors

The use of the method of finite elements and incremental deformations entails certain approximations. Accordingly the numerical solution of the mathematical problem differs from the exact analytical solution* . It is the purpose of this section to indicate briefly the sources of errors and to show how estimates of their magnitudes may be obtained.

*In addition it must be recalled that the exact solution of the mathematical problem would differ from the performance of the real material because of the approximations in the mathematical model.

(i) Errors due to the finite element method

Approximations made in the finite element method involved discretizing the displacement field and assuming a linear displacement field in each element. The nodal displacements are then evaluated by satisfying equilibrium conditions in an average sense through the use of a variational principle.

The accuracy of the method depends heavily on the selection of number, size and location of the elements. For two-dimensional problems in linear elasticity, the convergence obtained by increasing the number of elements has been demonstrated numerically by Clough[3] and McCormick[4]. Assessment of the errors incurred by the finite element method can only be made intuitively. Numerical solution of problems which have known analytical solutions and subsequent comparison of results gives a better background for such an intuitive assessment.

(ii) Errors due to linearization of the incremental stress-strain relations

In deriving the linear incremental stress-strain relations, Eq. (13), the second order terms in the strain increments were neglected in Eq. (12). In particular this implies, for example, that

$$\lambda >> |B_2 \, \Delta\epsilon_{mm}|$$

or in general that

$$\frac{|B_m \, \Delta\epsilon_{ij}|}{\lambda} << 1 \tag{43}$$

and where $|\ |$ denotes the absolute magnitude. From Eq. (43) it is clear that the increment size depends on the magnitude of the material constants.

Omitting the second order terms is equivalent to choosing a modulus K_A which is tangent to the stress-strain curve at the beginning of the increment (see Figure 8). The tangent modulus either overshoots or undershoots the exact result in each increment. After a number of successive increments the accumulated error may cause a significant departure from the exact solution.

One obvious way of reducing the error is to reduce the size of increment. In the next section a simple example is presented to demonstrate this point and at the same time indicate a suitable increment size.

The number of sequential problems that must be solved is inversely proportional to the size of increment. For this reason it is desirable to have a technique for improving accuracy which does not significantly increase the computational time. One such possibility is an iteration process, which may proceed in the following way.

The incremental problem is first solved with an initial tangent modulus K_A as before. Based on this solution, a close estimate of the average strain state may be obtained. The modulus K_B determined from the average strain state may be used to solve the incremental problem once again. As seen in Figure 8, the modulus K_B is a close approximation to the secant modulus in the increment. This iterative approach only doubles the number of linear problems to be solved and it might be expected to lead to a more accurate result than could be achieved by simply dividing the increment size by two.

(iii) Errors due to material instability

As pointed out in § III. 3, the second order model exhibits a material instability. Ordinarily, the second order law is not used up to strains high enough so that this instability is reached. However, in many problems in deformation analysis, localized high stress or strain gradients are induced such that small portions of the material experience large strains while the major portion of the material is subjected to strain states at a relatively low level. An example of such a problem is a loaded rigid footing resting on a sand foundation.

In applying the finite element-incremental deformation solution method it is expected that, if a small percentage of the elements attain the point of material instability, the overall solution will not be seriously affected. Consequently, as the incremental solution process used here proceeds, all of the elements are continually checked by Eq. (21) to determine if the material is stable. Should any of these inequalities be violated, the material matrix [D] from the previous increment (when the material was stable) is used to represent the behavior of that element for any subsequent deformation. In this way the possibility of numerical instability is avoided.

Once the numerical solution is completed, the number of elements that have surpassed the stability point and the stage when each reached this point is known. Based on this information, the overall applicability of the solution can be assessed. In the event elements are only affected in a localized region, St. Venant's principle would imply that the errors induced in the entire problem are restricted to the immediate vicinity of these elements.

5. A Simple Example With Different Load Increments

To develop intuition as to the necessary size of the increments, a simple example is considered. This example is the same as the plane strain pure shear test outlined in § III. 4. A hydrostatic compressive state $b_o = 7\times10^{-4}$ is first enforced. A state of pure shear strain

$$\delta\epsilon_{11} = -\epsilon$$
$$\delta\epsilon_{22} = \epsilon$$
$$\delta\epsilon_{33} = 0$$
$$\delta\epsilon_{ij} = 0 \qquad i \neq j$$

is then superposed. The resulting exact relation between $\delta\tau_{11}$ and ϵ is given by Eq. (23a). This relation is plotted in Figure 9 for the values of the material constants appearing in Table 1 and for the strain range $0 \leq \epsilon \leq 40\times10^{-4}$. The exact curve shown in Figure 9 is the same as the theoretical curve of $\delta\tau_{11}$ given in Figure 3.

In addition the results predicted from Eq. (13) for successive linear increments are plotted in Figure 9 for increments of 2, 4, 8 and 32. The calculations were carried out by hand. Comparison of the exact and approximate curves indicates satisfactory agreement only for the largest number of increments. The iteration procedure would have been recorded as well. It turns out, however, that due to the nature of the equations for this example, the first iteration gives the exact result.

V. NUMERICAL EXAMPLE

A computer program has been developed utilizing the solution method outlined in § IV. 2 and IV. 3. To illustrate its application to the stress analysis of granular materials, a numerical example is presented in this section.

1. Plane Strain Version of the Conventional Triaxial Test

A plane strain specimen of rectangular cross section (4a by 2a) is loaded by rigid platens as shown in Figure 10. The platen-soil interface is assumed to remain continuous throughout the test. The soil material is represented by a second order stress-strain relation with material constants as given in Table 1.

The specimen is first subjected to a uniform hydrostatic strain state

$$\epsilon_{xx} = \epsilon_{yy} = -7\times10^{-4}$$

$$\epsilon_{xy} = \epsilon_{xz} = \epsilon_{yz} = \epsilon_{zz} = 0$$

Normal forces, P, are then applied to the rigid platens causing overall compression in the material. It is the purpose of the analysis to determine the load-platen displacement relation as well as the stress field within the specimen.

Due to the symmetry of the problem, it is only necessary to consider one quadrant of the specimen. This quadrant is subdivided into 282 elements with 170 nodal points as shown in Figure 10. In anticipation of the character of the stress field the element size is reduced at the platen-soil interface and corner of the specimen.

Instead of dividing the load P into increments the platen deflection $v(x, 2a)$ is incremented. After determining the stress field for each increment of platen displacement, the corresponding incremental load ΔP is readily determined from statics. The platen displacement increment is taken to be $\Delta v(x, 2a) = -10^{-3}a$ which corresponds to an average compressive strain in the specimen of -5×10^{-4}. This increment size was selected after a careful study of a related but simpler problem. Its adequacy was further checked by further dividing the increment in two and comparing results for a limited portion of the loading path.

For numerical purposes it was found convenient to change the material stability criterion slightly. In this problem Eqs. (21) were replaced by

$$D_{11} > 100 \quad , \qquad D_{22} > 100 \quad , \quad D_{33} > 100$$

$$D_{11}D_{22} - D_{12}^2 > 100 \, , \quad D_{22}D_{33} - D_{23}^2 > 100 \, , \quad D_{11}D_{33} - D_{13}^2 > 100 \tag{44}$$

This altered form is used to ensure numerical stability. In the form given, Eqs. (44) are not properly normalized. Dividing both sides of the inequality by λ gives, for example

$$\frac{D_{11}}{\lambda} > \frac{100}{\lambda} = \frac{1}{46} > 0$$

From this normalized form it is clear that Eqs. (44) closely approximate the inequalities given by Eqs. (21).

The problem was numerically solved for eighteen successive increments*. At the end of the last increment a platen displacement of

*The running time on an IBM 7094 was 30 seconds per increment for a total of nine minutes.

$v(x, 2a) = -0.018a$ (0.9% average vertical strain) had been achieved and all of the elements had exceeded the modified material stability criterion, Eqs. (44). The resulting load-platen displacement curve is presented in Figure 11. It should be noted that the terminal slope of the load-deflection curve is slightly greater than zero, because of the use of the modified stability criterion. The same problem was solved again with increments of half the previous size (i.e. $-0.5 \times 10^{-3} a$) up to $v(x, 2a) = -0.012a$, in a study of increment size. The load-platen displacement curve was indistinguishable from that of Figure 11.

It will be noticed that, on Figure 11, the maximum value of axial load is very nearly reached at an axial strain of 0.75%. Since this example is a plane strain equivalent of the conventional soil triaxial test, and since it uses material properties derived from the behavior of a real soil in a testing apparatus, it might be expected that a more realistic strain (several percent) might have been realized from the computations. That this is not the case arises from the nature of the material stability criterion which had to be imposed because of the parabolic stress-strain law used. It is seen in Figures 3 and 5 that the theoretical principal stress-strain curve reaches a peak at a relatively small value of strain, whereas the experimental curve shows no peak in either test. This means that the numerical solution under discussion artificially limits the stress attainable in any element (through the stability criterion) to a value lower than the real soil may reach. Thus the effect of the cumulative stresses in elements — the axial load — is also truncated.

In practical problems, such as the computation of stresses and strains in the soil under a foundation, it should be pointed out that in a majority of

cases, the mass of the soil will be subjected to small strains in the range studied in the present example. If the behavior at larger strains is to be examined, the material constants may well be chosen so that the peak of the theoretical stress-strain curve occurs in a more realistic position with respect to the soil's behavior, even though the small strain representation may thereby be worsened. More study of this point has to be made.

In Figure 12 the element distribution in the specimen corner is presented and the elements in the shaded region are numbered. This numbering corresponds to the order in which they exceeded the stability criterion*. The points at which the stability criterion was exceeded for various elements are also indicated in Figure 11.

At a platen displacement of $v(x, 2a) = -0.015a$ only fourteen elements had surpassed the stability point. These fourteen elements are indicated in Figure 12 by shading. It is seen that only a small percentage of the specimen has violated the stability criterion. Accordingly, it is expected that the solution is satisfactory up to this point. Any subsequent loading of the platens causes extensive violation of the stability postulate thereby inducing significant errors in the result as discussed in § IV.4. While the numerical solution is satisfactory up to $v(x, 2a) = -0.015a$, the results still have to be assessed in light of the accuracy of the mathematical model. For this particular material the second order constitutive law only approximates the real material for a limited strain range. However, the

*Note that once an element exceeds the material stability point the material properties from the previous increment are used for all succeeding calculations, for that element.

numerical results were completed for a larger strain range to illustrate the severe nonlinearity that can be successfully predicted by the solution technique.

A linear finite element solution of the same problem was also solved for comparison purposes. It should be observed that this solution is not obtained by using simply the λ and μ values of the nonlinear material solution, since the problem studied commences at a given hydrostatic strain.

In Figure 13 the normalized normal interface stress is plotted and compared with the linear elastic result for the same axial strain, 0.75%. The two results do not differ markedly and both exhibit the high stress gradient in the vicinity of the specimen corner.

Figure 14 presents the interface shearing stress also for $v(x, 2a) = -0.015a$ at the same load P_o. The solution for a linear material is included for comparison. In both figures the stresses for the nonlinear material are slightly higher than their elastic counterparts in the central region of the specimen. Close to the corner, however, the elastic results exceed the predicted stresses for the nonlinear material as would be expected.

VI. DISCUSSION

From § III it is clear that the second order constitutive law can qualitatively predict some of the essential features of granular materials. As seen though from Figures 2, 3, 4 and 5, the accuracy is not good and range of applicability somewhat limited.

Several alternatives present themselves. The simplest extension involves the use of a higher-order polynomial in the stress-strain relations.

A third- or fourth-order constitutive law requires more work to evaluate the unknown material constants, but might lead to a significant improvement in the range of applicability.

It is not necessary to deal with polynomial expansions of the "strain energy density function." The pseudo-strain energy could be approximated by a variety of suitable functions. The selection of such functions might proceed on a trial and error basis, or stem from a detailed analysis of the particle mechanics of granular materials. In either case, should a proper function be determined, the material characterization is completed with only a minimum of curve fitting.

One of the chief difficulties encountered in the study outlined herein is the material instability in the second order stress-strain law. A possible way of circumventing this problem is to develop a second order strain-stress relation. In a manner similar to that leading to Eq. (6), it may be determined that

$$\epsilon_{ij} = \phi_o \delta_{ij} + \phi_1 \tau_{ij} + \phi_2 \tau_{i\ell} \tau_{\ell j} \tag{45}$$

where

$$\phi_i = \phi_i(J_1, J_2, J_3)$$

and

$$J_1 = \tau_{ii}$$

$$J_2 = \frac{1}{2} \tau_{ij} \tau_{ji}$$

$$J_3 = \frac{1}{3} \tau_{i\ell} \tau_{\ell j} \tau_{ji}$$

Proceeding as before, a second order strain-stress law is readily developed. The analog of Eq. (17) then becomes

$$\epsilon_I = C'_o + C_1'\tau_I + C_2' \tau_I^2 \qquad (46)$$

where C'_o, C_1', C_2' are functions of the material constants and principal stresses τ_{II}, τ_{III}. The one-dimensional curve represented by Eq. (46) is a parabola as before, but now it has a horizontal axis of symmetry. This means the material instability is now in a different quadrant and therefore Eq. (45) can better represent the character of a granular material. It should be pointed out that the plane strain formulation of the finite element procedure for a strain-stress relation is a little more difficult than that outlined in § IV. 2.

No matter how the deformation law is determined, it still suffers from a number of inherent disadvantages. The only way to obtain a constitutive law universally applicable to all strain-paths is to abandon the deformation law altogether and develop an appropriate incremental stress-strain law of plasticity.

Development of such a constitutive law requires an extension of current incremental plasticity laws to account for kinematic strain hardening, dependence on the hydrostatic state, nonlinear elastic hydrostatic stress-volume change as well as shear-dilatancy interaction. The experimental work that must necessarily parallel these analytical improvements is a formidable task.

It was the purpose of this study to consider first a deformation law as only a first approximation to the real material behavior. The numerical solution method developed was based on the incremental stress-strain law derived from the deformation law. Naturally, this same solution method is equally applicable to an incremental law based on the foundations

of incremental plasticity.

Finally,it should be pointed out that the results obtained in this study were a result of a unified effort by several people with different interests. The research required a blending of portions of several disciplines — soil mechanics, numerical analysis, material experimentation and applied mechanics. The authors feel that such a simultaneous joint effort proceeded considerably more efficiently and successfully than independent investigations would have done.

VII. ACKNOWLEDGMENTS

The research outlined here was undertaken under NSF Grant GK-626 in the Division of Engineering and Applied Science at the California Institute of Technology. This work forms a part of a general investigation into constitutive relations for soils and their use in practical problems. This research grant is under the general supervision of Professor R. F. Scott.

A portion of the participation by Dr. R. A. Westmann was supported by the College of Engineering, University of California, Los Angeles, California.

LIST OF FIGURES

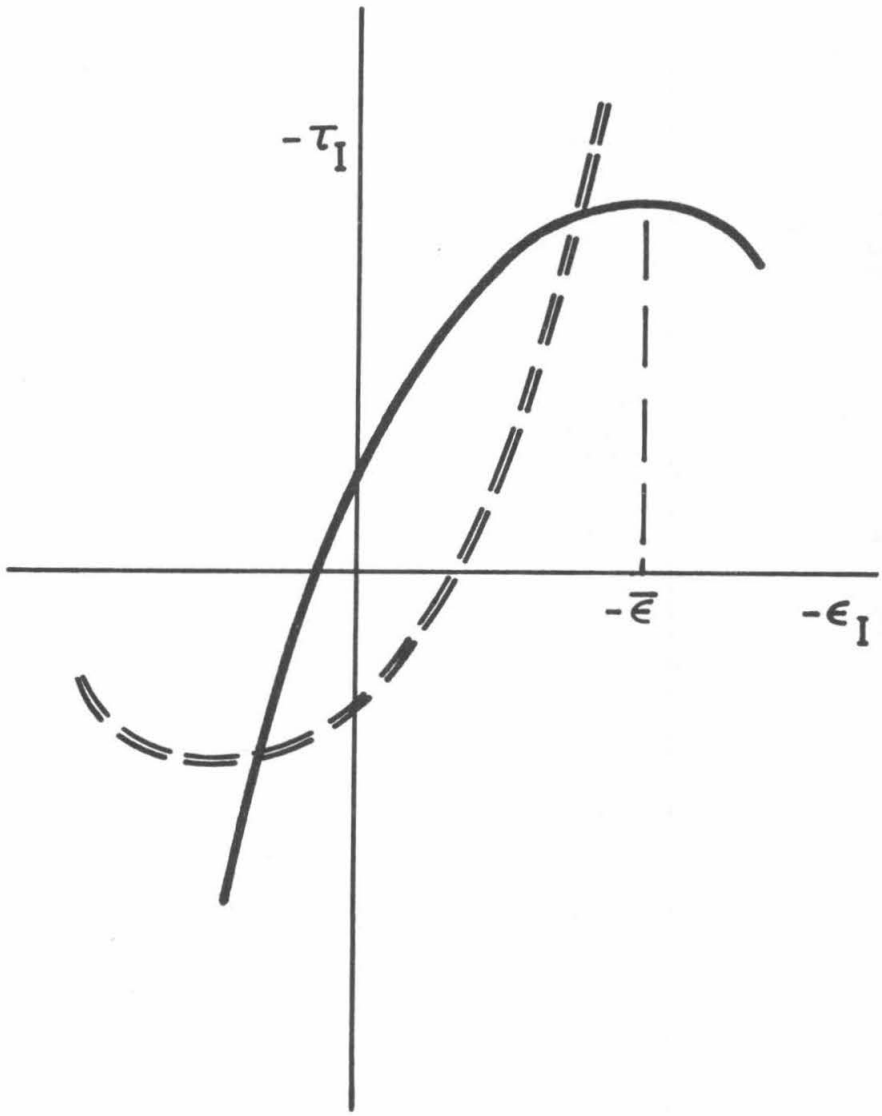

Figure 1. Parabolic nature of stress-strain curve in second-order law representation of one-dimensional test.

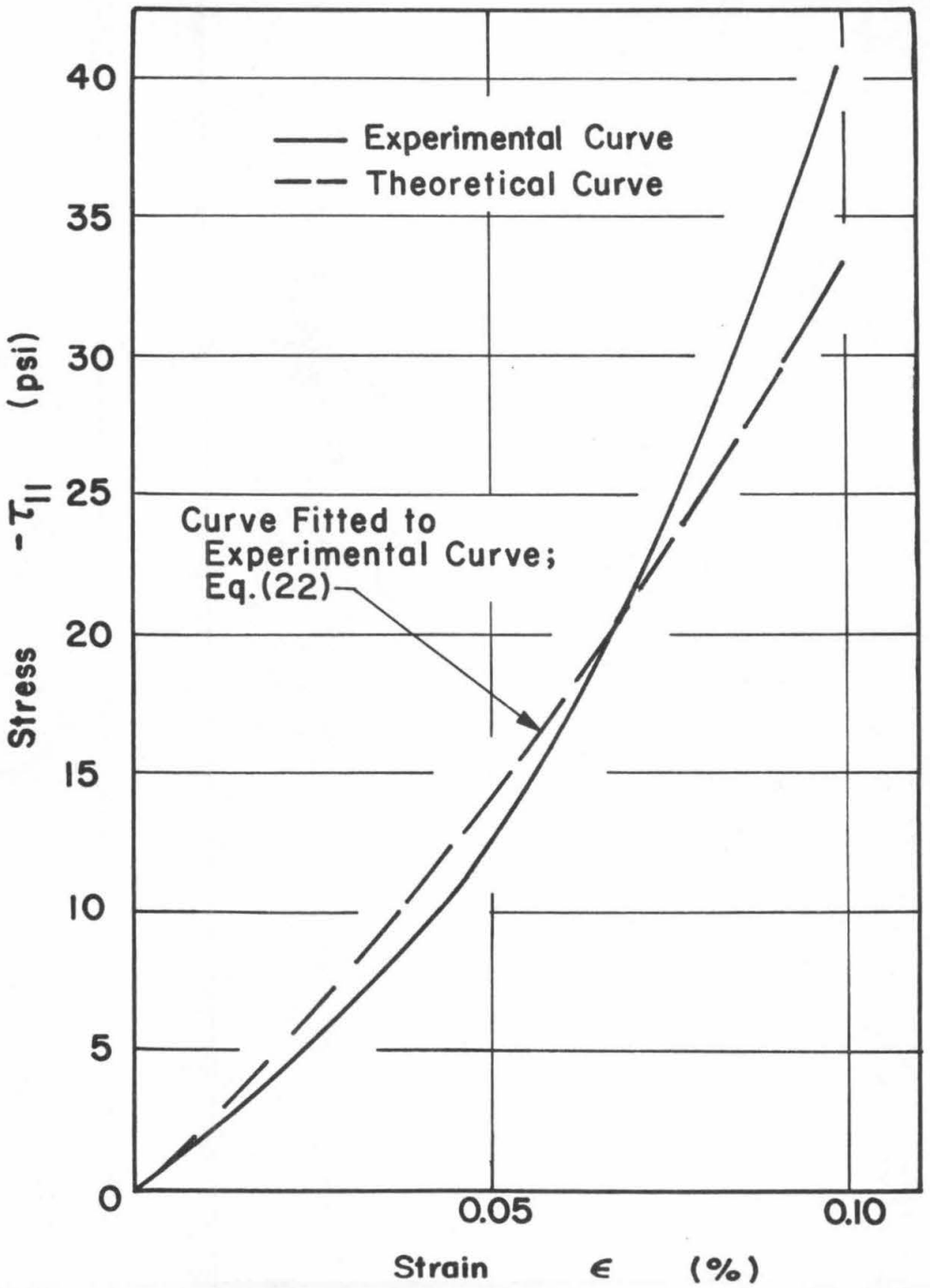

Figure 2. Hydrostatic compression test.

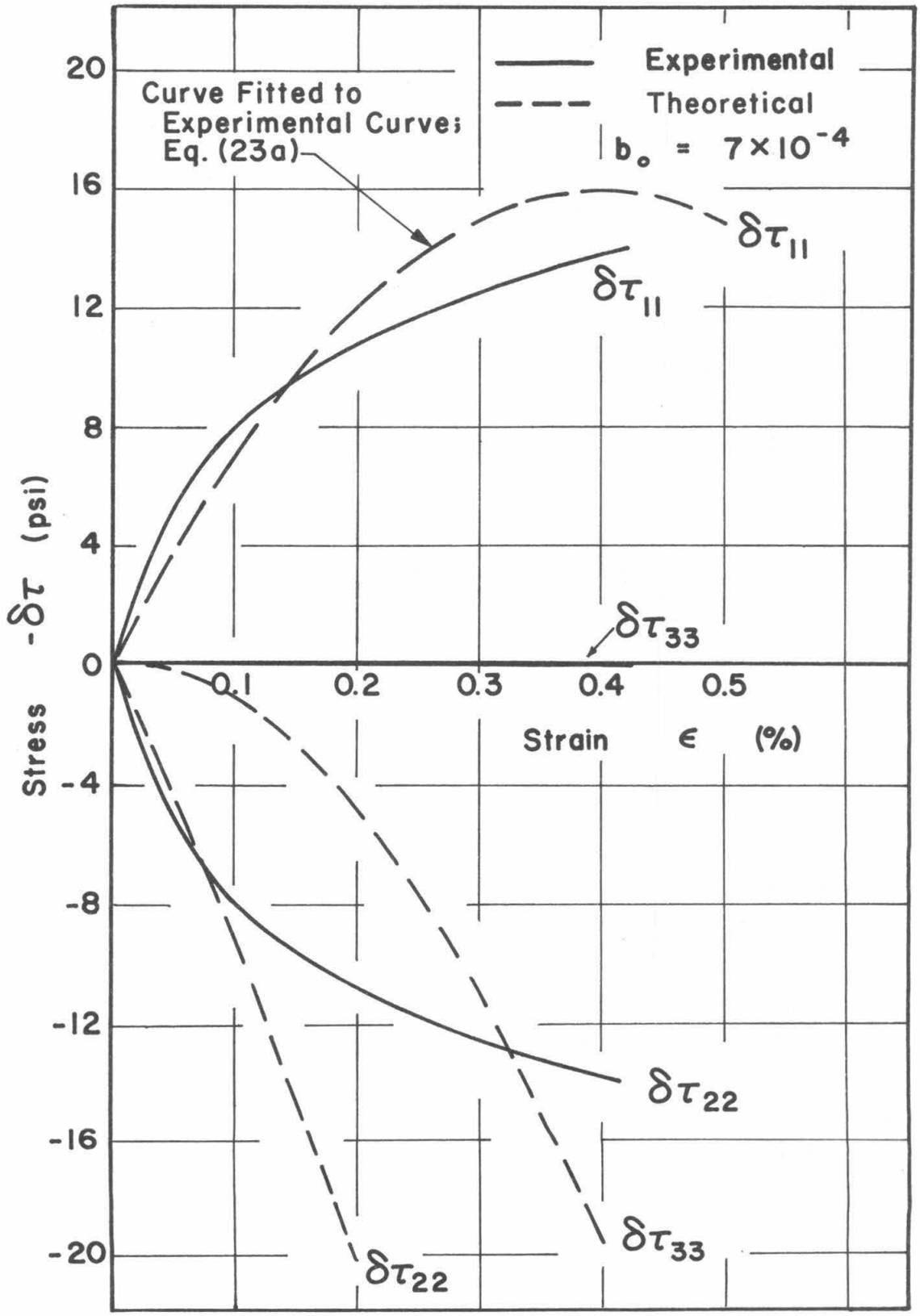

Figure 3. Simple shear test from an initial hydrostatic state.

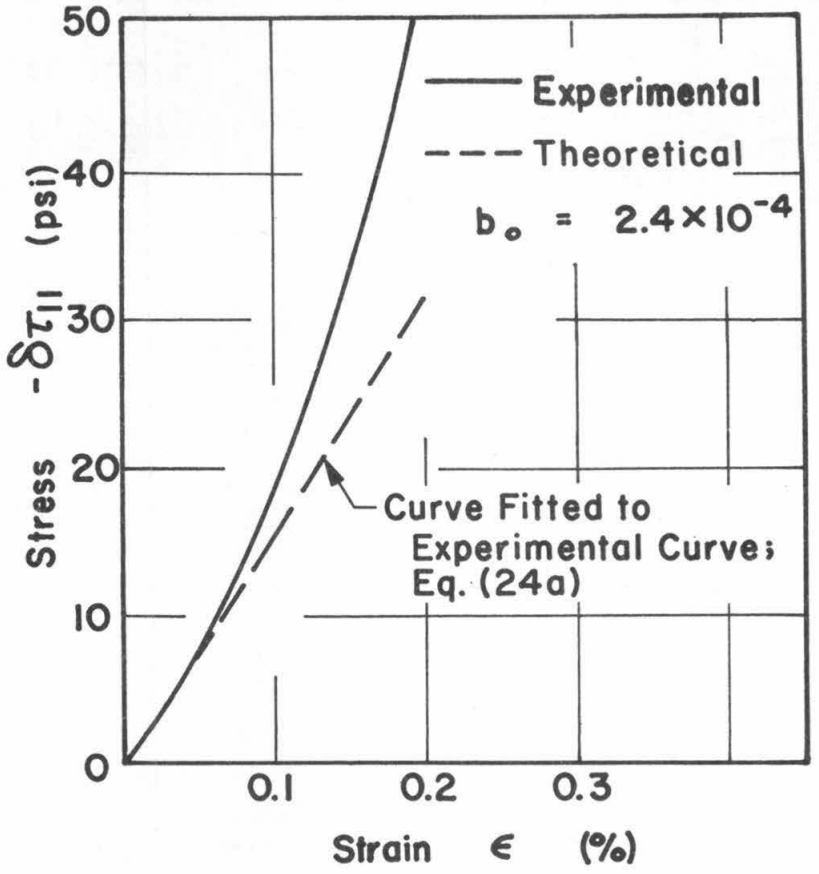

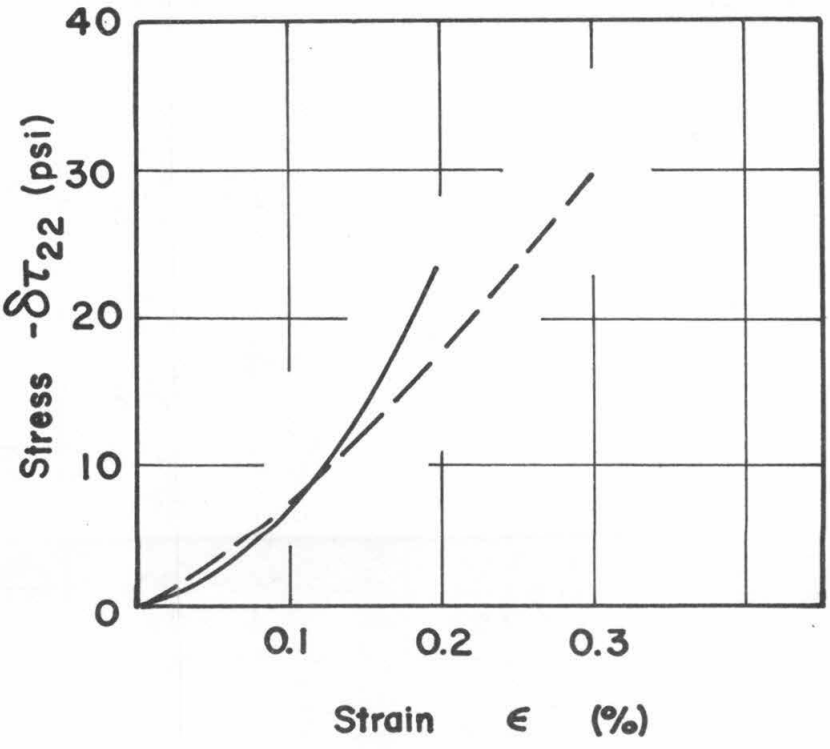

Figure 4. One-dimensional compression test.

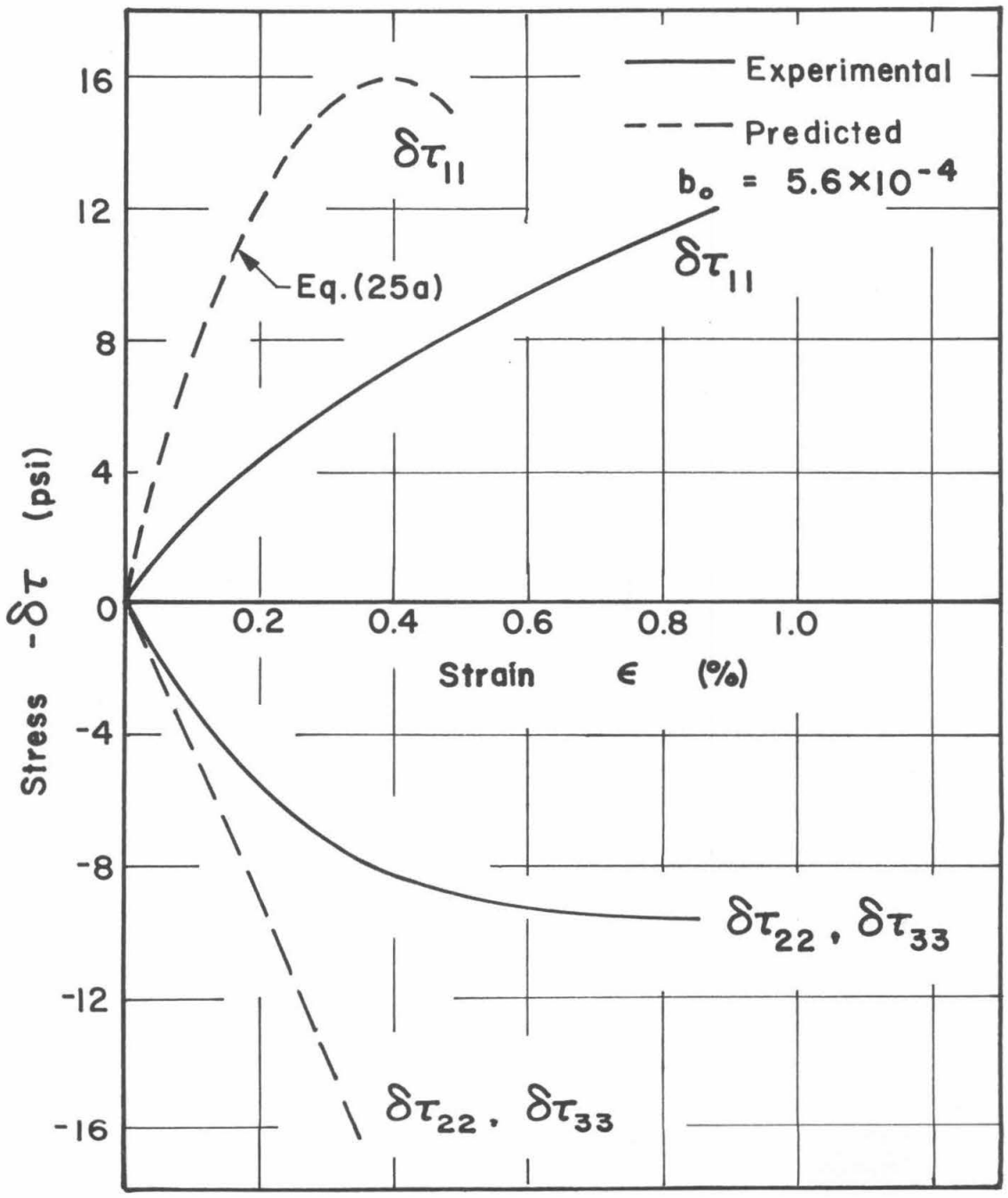

Figure 5. Triaxial shear test.

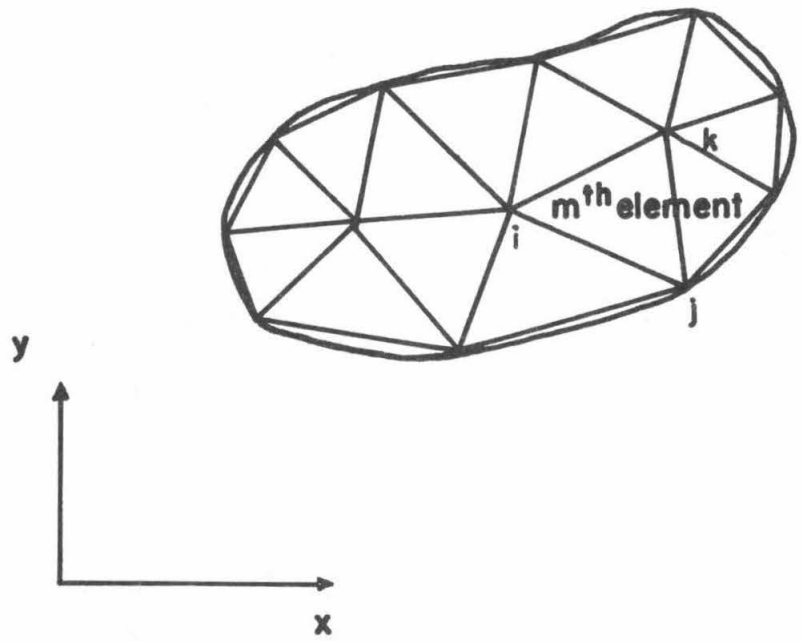

Figure 6. Subdivision of region into discrete elements.

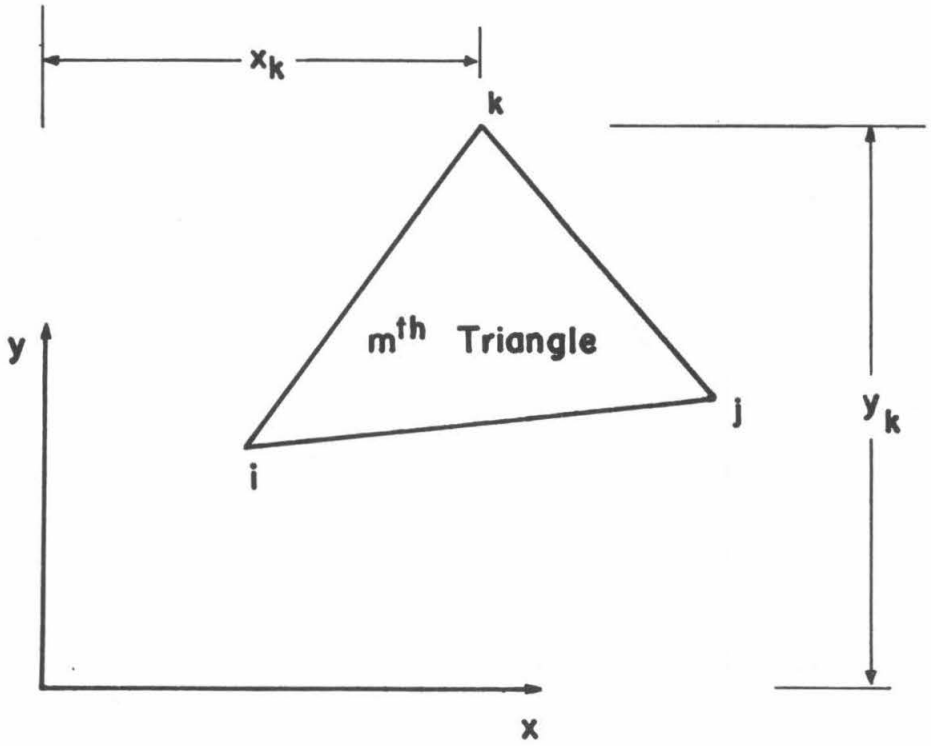

Figure 7. Single triangular element.

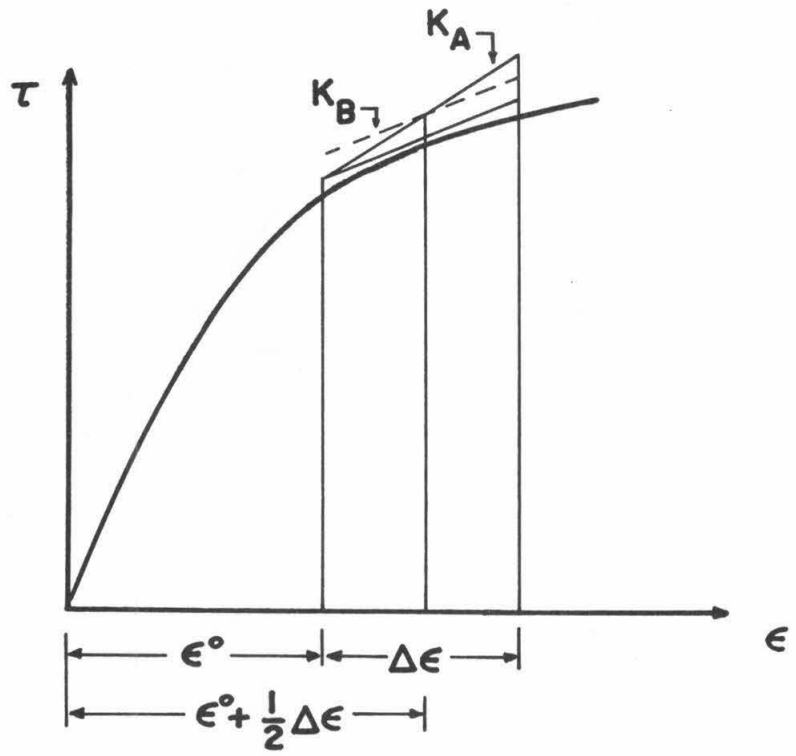

Figure 8. Incremental tangent and secant moduli.

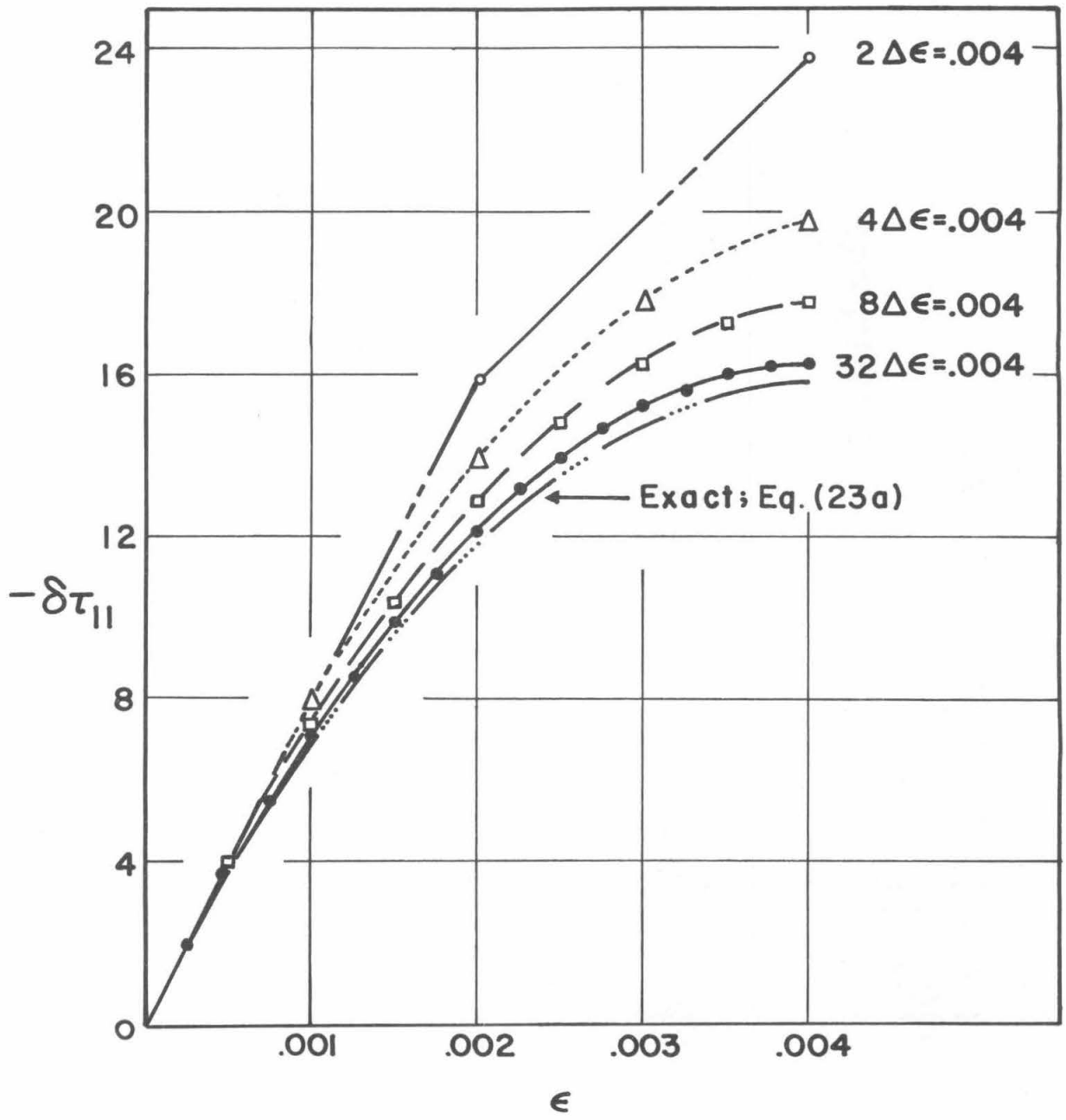

Figure 9. Comparison of incremental analysis of plane strain pure shear test with exact solution.

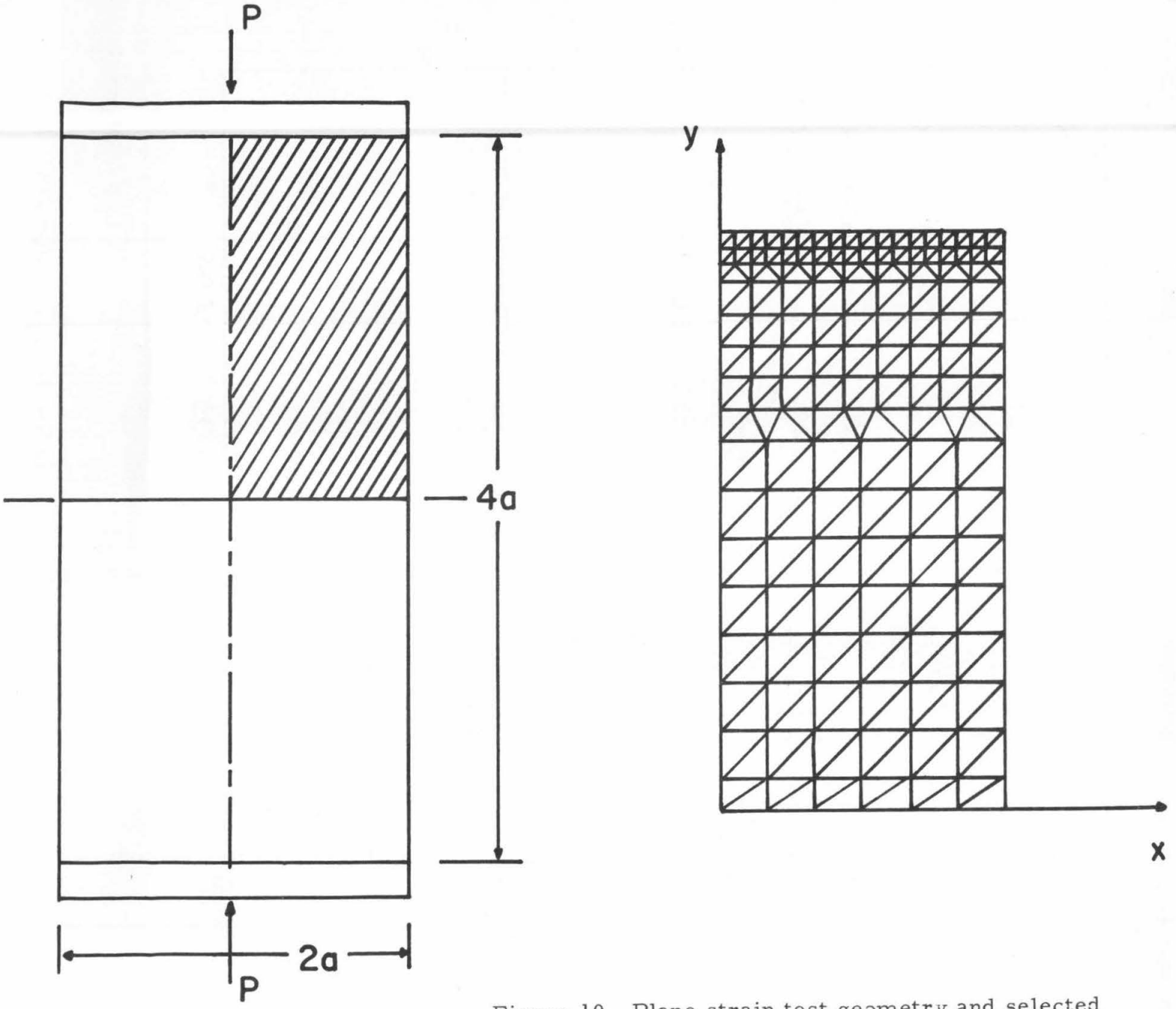

Figure 10. Plane strain test geometry and selected distribution of finite elements.

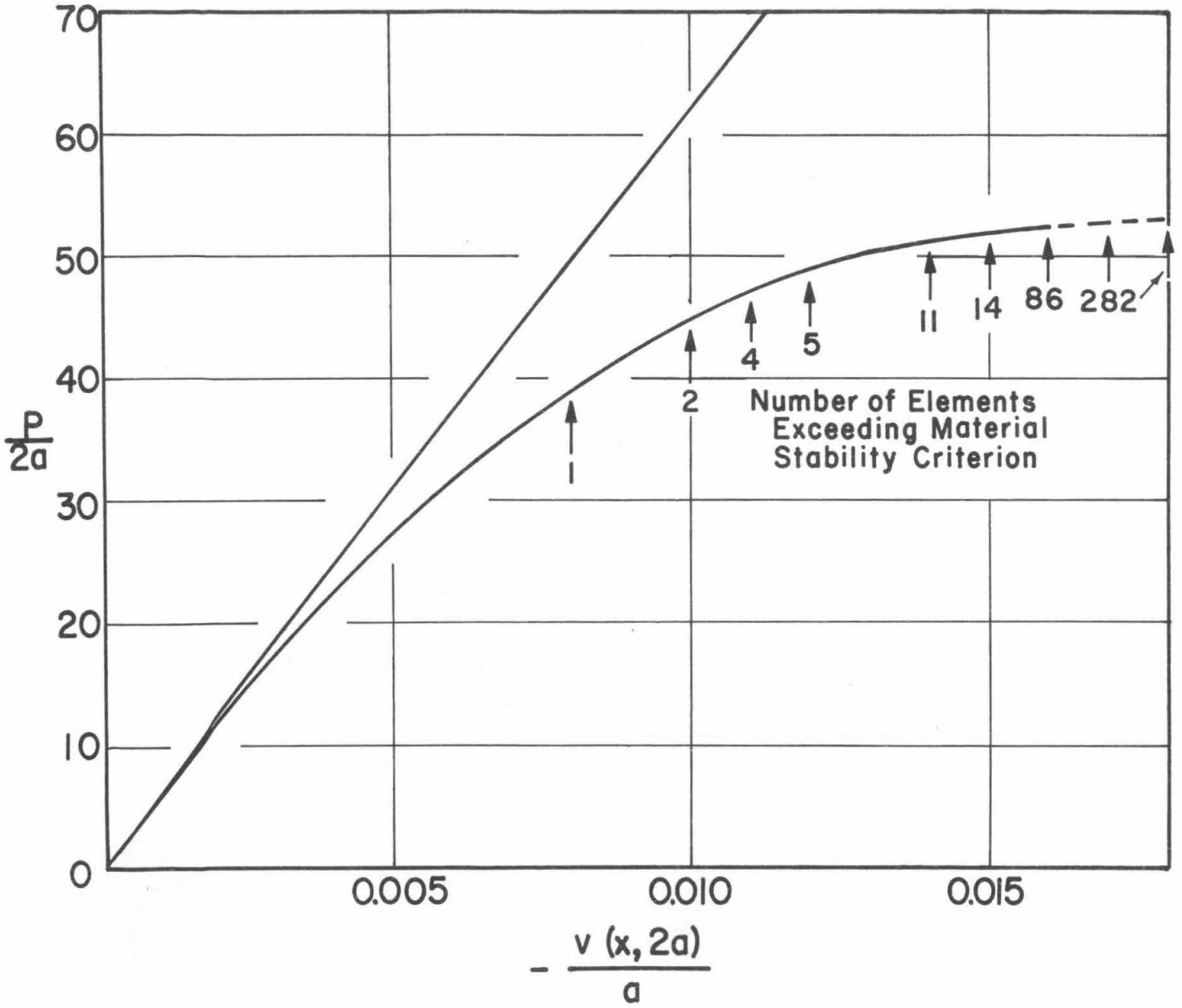

Figure 11. Computed average axial stress-strain curve for plane strain test.

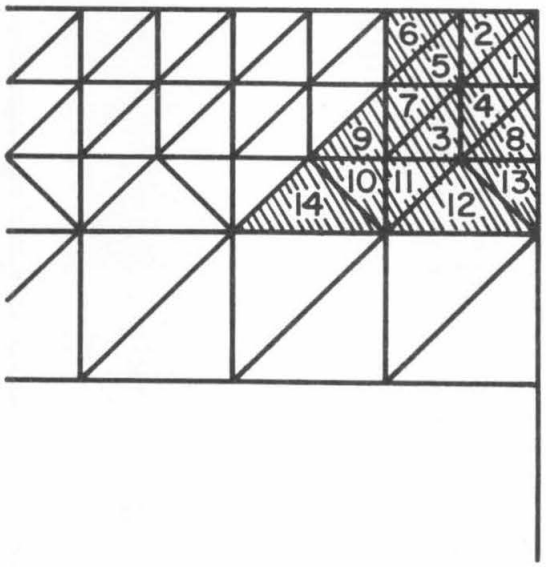

Figure 12. Order in which corner elements reach stability criterion.

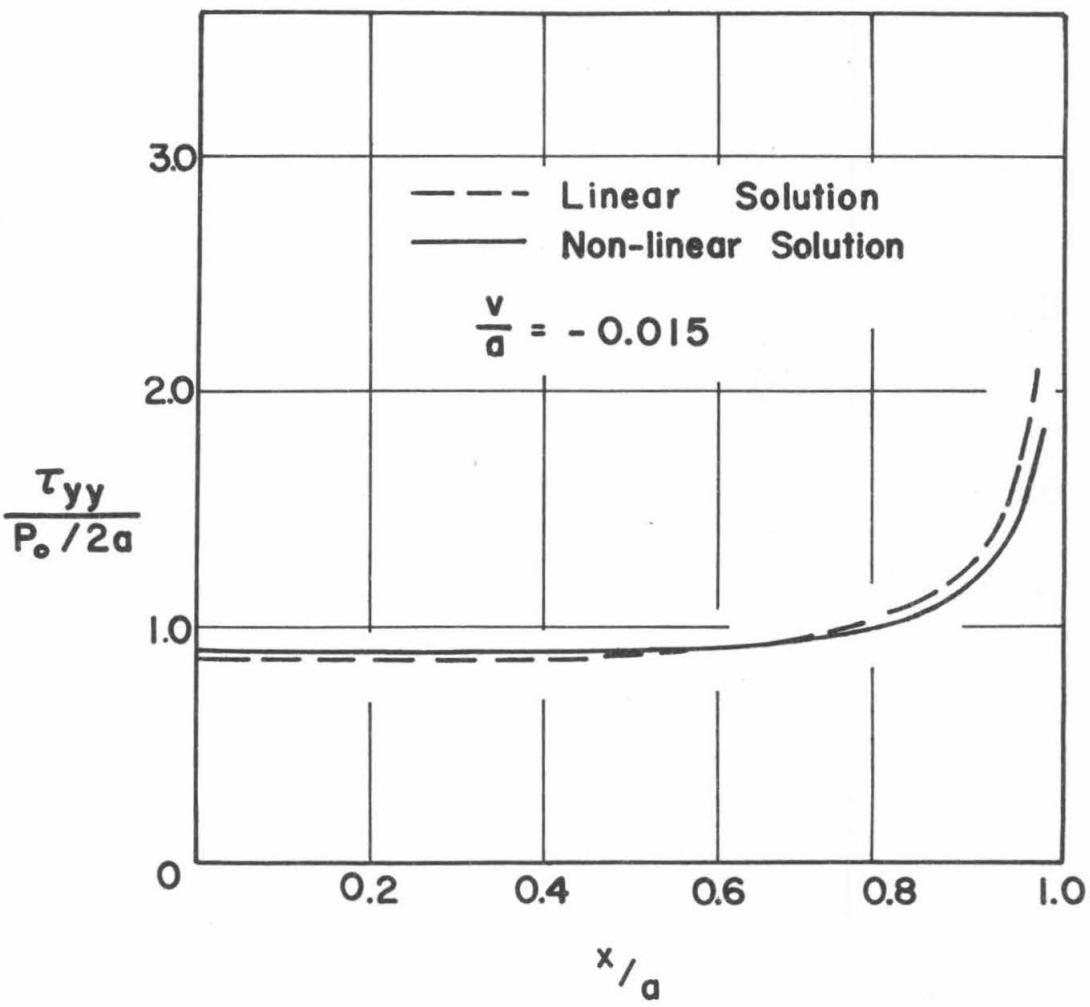

Figure 13. Comparison of normal interface stresses for linear and nonlinear materials in plane-strain test.

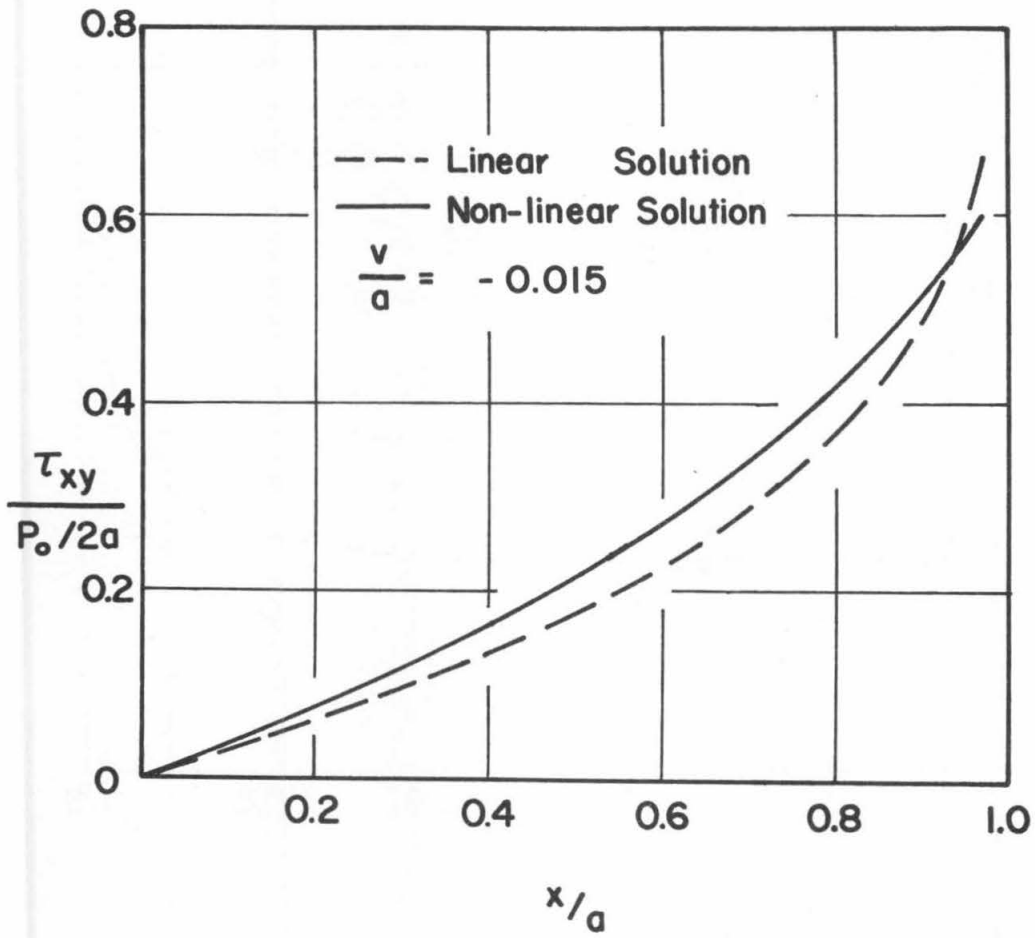

Figure 14. Comparison of shearing interface stresses for linear and nonlinear materials in plane-strain test.